https://doi.org/10.5194/acp-2020-798
Preprint. Discussion started: 17 September 2020

Atmospheric Chemistry and Physics Discussions

Temperature and acidity dependence of secondary organic aerosol formation from α-pinene ozonolysis with a compact chamber system

Yange Deng[1], Satoshi Inomata[1]*, Kei Sato[1], Sathiyamurthi Ramasamy[1], Yu Morino[1], Shinichi Enami[1], Hiroshi Tanimoto[1]

[1]National Institute for Environmental Studies, Tsukuba 305-8506, Japan

Correspondence to: Satoshi Inomata (ino@nies.go.jp)

Abstract. Secondary organic aerosol (SOA) is of great importance, affecting human health and the prediction of climate change; however, the factors (e.g., temperature, acidity of pre-existing particles, and oxidants) influencing its formation are not sufficiently resolved. In this study, a compact Teflon atmospheric simulation chamber is developed, in which reactions in atmospheric pressure conditions can be performed with controlled temperature, humidity, oxidation agents, and seed particle acidity. Using the chamber, α-pinene ozonolysis SOA formation was simulated under temperatures of 278 K, 288 K, and 298 K with neutral/acidic seed aerosols. The SOA components of *m/z* less than 400 were analyzed using negative electrospray ionization liquid-chromatography time-of-flight mass spectrometry. The temperature and acidity dependence of SOA yields and chemical components were investigated. From the slightly negative temperature dependence of the SOA yields, the enthalpy of vaporization in neutral and acidic seed conditions was estimated to be 25 and 44 kJ mol^{-1}, respectively. With these values, the volatility distributions of the identified SOA compounds were consistently explained. Acidity dependence analysis of the chemical formula, molecular mass, and O:C ratio of the detected compounds indicated the enhanced formation of many oligomers in the wide molecular mass range with a wide range of O:C ratios under acidic seed conditions. The acidity dependence of certain major compounds could be explained by acid-catalyzed heterogeneous reactions (e.g., m/z 171, 185, 343, and 357) or acid-catalyzed decomposition of hydroperoxides (e.g., m/z 215 and 197). In addition, the formation of organosulfates (OS) was observed under acidic seed conditions. We proposed that six of the eleven detected OS were possibly formed through the aldehyde + HSO_4^- pathway. Further studies on the OS formation during α-pinene ozonolysis are warranted.

1 Introduction

Secondary organic aerosol (SOA) in the atmosphere is a complex of organic compounds which are formed through photooxidation of precursor volatile organic compounds (VOCs) of either biogenic (e.g., monoterpene and isoprene) or anthropogenic (e.g., alkanes and aromatics) origins, or both (Hallquist et al., 2009). SOA plays important roles in the aerosol effect on climate (Tilmes et al., 2019), air quality (Parrish et al., 2011), as well as human health (Shiraiwa et al., 2017). Nevertheless, it is noted in the IPCC Fifth Assessment Report (AR5) that the formation of SOA has not been included in the estimation of the radiative forcing from aerosols because the formation is influenced by a variety of factors not yet sufficiently quantified (Stocker et al., 2013). However, in association with the advance of research technologies, processes that influence the growth of SOA particles to sizes relevant for clouds and radiative forcing have been intensively investigated (Shrivastava et al., 2017).

The importance of the formation of low volatility organic compounds (LVOCs) with saturate concentrations of less than $10^{-0.5}$ μg m^{-3} has been highlighted in the SOA formation mechanisms of recent studies (Ehn et al., 2014; Shrivastava et al., 2017). Semi-volatile organic compounds (SVOCs) are generated from oxidation reactions of VOCs in the gas phase. Heterogenous/multiphase reactions of SVOCs on particles are thought to contribute to the formation of LVOCs in SOA. Earlier acid-catalyzed heterogeneous reaction studies (Jang et al., 2002; Hallquist et al., 2009) proposed the formation of hemiacetals,

https://doi.org/10.5194/acp-2020-798
Preprint. Discussion started: 17 September 2020

Atmospheric Chemistry and Physics Discussions

aldol products, organosulfates, among others, in the presence of acidic seed particles, which prompted the notion that the acidity of pre-existing particles is one of the key factors that influence SOA formation.

The influence of the acidity of pre-existing particles on SOA formation has been investigated in both chamber experiments and field measurements. From chamber experiments, Eddingsaas et al. (2012) observed the clear uptake of several SVOCs (e.g., α-pinene oxide and α-pinene hydroxy hydroperoxides) after the injection of acidic particles into α-pinene OH oxidation system under low-NOx conditions (photooxidation for four hours, lights off and contents in the dark for two hours followed by the injection). However, no apparent uptake was observed after the injection of neutral particles. Shiraiwa et al. (2013a) observed the evident formation of peroxyhemiacetals after gaseous tridecanal was injected into the dodecane photooxidation system under dry, ammonium sulfate seed particles, and low-NOx conditions (photooxidation for four hours, lights off and contents in the dark for two hours followed by the injection), which was believed to have been catalyzed by the presence of acids generated in the low-NOx dodecane mechanism. However, contrary results have been reported for the influence of the acidity of pre-existing particles on SOA yields from chamber experiments. For example, whereas Offenberg et al. (2009) reported a positive relationship between the acidity of seed particles and the ratio of SOA concentrations from the photooxidation of α-pinene with NOx at an elevated acidity relative to neutral seed conditions, Eddingsaas et al. (2012) reported greater SOA yields under acidic than neutral seed conditions from photooxidation of α-pinene under high-NOx conditions, and no influence of seed particle acidity under low-NOx conditions. Field studies also reported contrary results on the influence of acidity on SOA formation. Some researchers reported that SOA formation was enhanced under more acidic conditions (Chu et al., 2004; Lewandowski et al., 2007; Zhang et al., 2007; Hinkley et al., 2008; Renjarajan et al., 2011; Zhou et al., 2012), whereas others reported little or no enhancement under acidic conditions (Takahama et al., 2006; Peltier et al., 2007; Tanner et al., 2009). Other factors, such as temperature, humidity, NO_x concentration level, and oxidation agents, might have also affected the results of the aforementioned studies in addition to the acidity of pre-existing particles (Jang et al., 2008), but they also are not well understood. This motivated the current study to develop a new compact chamber system, in which SOA formation reactions under controlled temperature, humidity, oxidation agents, and seed particle acidity can be easily performed.

Monoterpenes are known to be a large source of SOA in the global atmosphere (Kelly et al., 2018). α-Pinene is the dominant monoterpene and the second-most emitted VOC following isoprene (Guenther et al., 2012; Messina et al., 2016). It can react rapidly with atmospheric oxidants including O_3, OH, and NO_3 radicals, and ozonolysis is the major atmospheric oxidation pathway, which is estimated to account for 46 % of reacted α-pinene (Capouet et al., 2008). Pre-existing studies regarding α-pinene ozonolysis indicate that both SOA yields and chemical compositions in SOA are influenced by the air temperature and aerosol acidity (Czoschke et al., 2003; Gao et al., 2004; Iinuma et al., 2004, 2005; Czoschke and Jang, 2006; Jang et al., 2006; Northcross and Jang, 2007; Surratt et al., 2007, 2008; Hallquist et al., 2009; Saathoff et al., 2009; Kristensen et al., 2014, 2017). Pathak et al. (2007b) found that the SOA yields show a weak temperature dependence in the range of 15 to 40 °C and a stronger temperature dependence between 0 and 15 °C. Saathoff et al. (2009) parameterized the temperature dependence of the two-product SOA yield parameters using a dataset including several previous studies as well as their own comprehensive measurements from 243 to 313 K. In general, a negative temperature dependence of the α-pinene ozonolysis SOA yields could be confirmed. While enhancements of SOA yields from α-pinene ozonolysis reactions under acidic seed aerosol conditions compared with neutral seed conditions have been generally observed in previous studies (Czoschke et al., 2003; Gao et al., 2004; Iinuma et al., 2004, 2005; Czoschke and Jang, 2006; Jang et al., 2006; Northcross and Jang, 2007), the degree of enhancement varied. For example, the studies of Czoschke et al. (2003), Iinuma et al. (2004), Czoschke and Jang (2006), Jang et al. (2006), and Northcross and Jang (2007) reported enhancement ranges of 21–87 % from weak acid seed conditions to high acid seed conditions. Conversely, studies of Gao et al. (2004) and Iinuma et al. (2005) reported both increases and

https://doi.org/10.5194/acp-2020-798
Preprint. Discussion started: 17 September 2020

Atmospheric Chemistry and Physics Discussions

decreases of SOA yields under acidic seed conditions. The variety of the SOA yield differences between acidic and neutral seed conditions could probably be related to different experimental settings among the studies.

With respect to chemical compositions, Kristensen et al. (2017) compared the chemical compositions of α-pinene ozonolysis SOA formed at temperatures of 293 and 258 K and found that the mass fraction of carboxylic acids increased at 258 K compared to 293 K, while the formation of dimer esters was suppressed at the sub-zero reaction temperature. Compared with neutral seed conditions, enhanced formation of large molecules under acidic seed conditions has been reported by Gao et al. (2004) and Iinuma et al. (2004). Gao et al. (2004) additionally reported less abundant small oligomers (e.g., a compound with molecular mass of 358) under acidic seed conditions. Their research indicates that systematic studies of α-pinene ozonolysis SOA formation under specific experimental settings are warranted to clarify temperature and acidity dependence.

Furthermore, enhanced formation of organosulfates (OS) from α-pinene oxidation under acidic seed conditions has been suggested by previous studies (Surratt et al., 2007, 2008; Iinuma et al., 2009; Duporté et al., 2020). OS has been regarded as an important aerosol component, accounting for up to 30 % of organic mass in PM_{10}, and also as an anthropogenic pollution marker in the past two decades (Iinuma et al., 2007, 2009; Surratt et al., 2007, 2008; Riva et al., 2015, 2016; Duporté et al., 2016, 2020). The formation mechanisms of OS from α-pinene oxidations have been studied under different experimental settings. For example, Surratt et al. (2007) proposed OS formation through esterification of hydroxyl or carbonyl groups in photooxidation experiments. Surratt et al. (2008) proposed nitrooxy organosulfates formation through esterification of hydroxyl groups in nighttime oxidation (i.e., NO_3-initiated oxidation under dark conditions). Iinuma et al. (2009) proposed the acid-catalyzed ring-opening of epoxides mechanism through the α-pinene oxide/acidic sulfate particle experiment. Nozière et al. (2010) proposed a sulfate radical initiated process of α-pinene in irradiated sulfate solutions. For α-pinene ozonolysis experiments, the formation of OS through reactions between SO_2 and stabilized Criegee intermediates under dry conditions or organic peroxides in aqueous phase has been recently suggested (Ye et al., 2018; Stangl et al., 2019; Wang et al., 2019). However, based on our knowledge, no study concerning OS formation from α-pinene ozonolysis in the presence of sulfate particles exists.

In this study, α-pinene ozonolysis experiments have been conducted under dark conditions in the presence of seed particles and an OH scavenger. The study aimed to clarify the temperature and acidity dependence of the yield and chemical composition of α-pinene ozonolysis SOA. Moreover, OS compounds and its possible formation mechanisms have been targeted during the analysis.

2 Experimental

2.1 Chamber description and operation

A temperature-controllable chamber system has been developed for the simulation of SOA formation (Fig. S1). The chamber is a cuboid shape Teflon bag (FEP; 0.7 m^3 volume, 900 mm × 600 mm × 1300 mm; 50 μm thickness; Takesue, Japan) contained in a constant temperature cabinet (HCLP-1240; W1200 mm × D703 mm × H1466 mm; NK System, Japan). The chamber is collapsible and is operated in atmosphere pressure. For a typical experimental run, a total volume of more than 0.6 standard cubic meters (sm^3) G3 pure air (CO_2 < 1 ppmv, CO < 1 ppmv, THC < 1 ppmv, and dew temperature < −70 °C) with variable relative humidity (RH) was introduced into the Teflon chamber. The RH of the air was adjusted by passing the G3 pure air through MiliQ water (resistivity of 18.2 MΩ·cm) before entering the Teflon bag. α-Pinene liquid (Wako Chemicals, Japan) was injected into the G3 pure air line through a septum equipped in a Swagelock PFA Tee connector using a micro-syringe (ITO corporation, Japan) in the middle of the injection of pure air. Diethyl ether in nitrogen gas (mass fraction of 0.4 %; Takachiho, Japan) used as an OH radical scavenger was introduced to the chamber in excess amounts (approximately 53 ppmv; 164–1963 times the initial concentration of α-pinene) after the introduction of pure air. Seed aerosol particles generated by a

https://doi.org/10.5194/acp-2020-798
Preprint. Discussion started: 17 September 2020

Atmospheric Chemistry and Physics Discussions

commercial atomizer (ATM220S, TOPAS GmbH, Germany) were subsequently introduced into the Teflon chamber. Neutral seed aerosols were generated from a 0.6/0.3 mol L^{-1} $(NH_4)_2SO_4$ solution and acidic seed aerosols were generated using a solution mixture of 0.25 mol L^{-1} $(NH_4)_2SO_4$ and 0.25 mol L^{-1} H_2SO_4. After 30 min of stabilization, the initial concentrations of α-pinene and seed aerosols were measured with a quadrupole-type proton transfer reaction mass spectrometry instrument (PTR-QMS500, Ionicon Analytik Gesellschaft m.b.H., Innsbruck, Austria) and a scanning mobility particle sizer (SMPS, TSI classifier model 3082; differential mobility analyser model 3081; condensation particle counter model 3772; USA), respectively. The SMPS was contained in a smaller constant temperature cabinet (LP-280-E, NK System, Japan), whose temperature was adjusted to be the same as the cabinet containing the Teflon chamber. The sheath and sample flow rates of the SMPS were 3.0 and 0.3 L min^{-1}, respectively. The measured diameter range of the SMPS was 13.8–685.4 nm, and the data were collected every 5 min. After obtaining the initial concentration of α-pinene and seed aerosols, excess ozone produced by irradiation of pure O_2 with vacuum ultraviolet light from a low-pressure mercury lamp ozone generator (Model 600, Jelight Compony Inc., USA) was introduced into the chamber to start the ozonolysis reactions. The ozone concentration in the chamber was measured with an ozone monitor (Model 1200, Dylec, Japan) immediately after its introduction. For some experiments, the order of the introduction of α-pinene and O_3 was inverted (see Tables S1 and S2). The concentrations of both the α-pinene and aerosols were continually measured until the end of the experiment, which is defined in this study as 90 min after the start of the α-pinene ozonolysis reaction. The concentration of ozone after 90 min of ozonolysis reactions was also measured. In total, 40 experimental runs were executed under neutral or acidic seed aerosol conditions at temperatures of 278, 288, or 298 K. For experiments with the same temperature setting, the RH settings were also similar (Tables S1 and S2). Notably, when the chamber temperature was set to 278 K, the temperature in the small cabinet was set to 280 K, which is the lowest work temperature of the SMPS. The Teflon bag was flushed with G3 pure air at least three times between two successive experimental runs, which took approximately 40 min.

One Teflon filter (PF020, 47 mm diameter, Advantec MFS) aerosol sample was collected for each different combination of seed and temperature condition. The sample volume was 0.5 m^3 for each sample. In total, six aerosol samples were collected, and they were subjected to negative electrospray ionization liquid-chromatography time-of-flight mass spectrometry analyses (Sect. 2.2). The acidity of the seed particles was measured in a separate experiment where the seed particles were sampled on a Teflon filter which was then extracted into 10 mL MiliQ water. The pH of the water solution was measured with a pH meter (FPH70, AS ONE, Japan). The H^+ concentration was ~220 nmol m^{-3} under the acidic seed conditions.

2.2 LC-TOF-MS analysis

Chemical composition analysis of the Teflon filter samples was conducted using electrospray ionization liquid-chromatography time-of-flight mass spectrometry (LC-TOF-MS) (Agilent Technologies, UK) similarly as in previous studies (Sato et al., 2018, 2019) except that negative-mode was used in this study whereas positive-mode was used in those previous studies. The mass calibration and lock-mass correction were conducted using G1969-85000 and G1969-85001 tuning mixtures (Agilent Technologies, UK), respectively. The mass resolution of the mass spectrometer (full width at half maximum) was > 20000. For the analysis, the Teflon filter sample was sonicated in 5 mL methanol for 30 min. The filter extract was concentrated to near dryness under a stream of nitrogen (~1 L min^{-1}). A 1 mL formic-acid–methanol–water solution (*v*/*v*/*v* = 0.05/100/99.95) was added to the concentrated extract to obtain the analytical sample. A 10 µL aliquot of the analytical sample was injected into the LC-TOF-MS instrument and separated with an octadecyl silica gel column (Inertsil ODS-3; GL Science, Japan; 0.5 µm × 3.0 mm × 150 mm). A formic-acid–water solution (0.05 % *v*/*v*) and methanol were used as mobile phases. The total flow of the mobile phases was 0.4 mLmin^{-1}. The methanol fraction during each analysis was set at 10 % (0 min), 90 % (30 min), 90 % (40 min), 10 % (45 min), and 10 % (60 min). As reported previously (Sato et al., 2007), the recovery of malic acid, whose saturation concentration was estimated to be 157 µg m^{-3}, was determined to be >90 %, suggesting that evaporation

https://doi.org/10.5194/acp-2020-798
Preprint. Discussion started: 17 September 2020

Atmospheric Chemistry and Physics Discussions

loss during pre-treatment is negligible for molecules with saturated concentrations of ~10^2 μg m^{-3} or less. We determined the chemical formulae and signal intensities for 362 products (including eleven organosulfates) of different m/z (Table S3).

2.3 Wall-loss experiments

The wall-loss rate of particles in the chamber was evaluated by measuring the time evolution of the volume-size distributions of seed-only particles using the SMPS. The measurements were carried out whenever a new Teflon bag was used or the experimental conditions (i.e., temperature or seed particle acidity) were changed under humid air conditions. The latest measured bulk wall-loss rate (Sect. 3.1) was applied for each SOA formation experiment.

In Fig. S2, size-resolved aerosol wall-loss rates, which were determined assuming first-order wall-loss constants (Wang et al., 2018a), were shown for seed particles of different size-distributions. Large wall-loss was observed for particles with mobility diameters of less than 100 nm, caused mainly by coagulation (Wang et al., 2018a). Large wall-loss for particles with mobility diameters of larger than 200 nm was also observed. This is a shortcoming of this chamber and could be explained by the shorter sedimentation time in the compact space compared with large chambers. Figure S2 also indicates that the wall-loss rates of super-200 nm particles were relatively high when the mean diameter of the seed particles was relatively small. Therefore, we waited for 30 min after the introduction of seed particles to start the ozonolysis reaction so that the size distribution of the seed particles could shift to the larger size end due to coagulation and loss of small particles. In addition, we used high concentration solutions for the generation of seed particles to produce large particles in this study (Sect. 2.1).

3 Data analysis

3.1 Derivation of SOA yield

SOA yield (Y) is defined as the ratio of the mass concentration of SOA (m_{SOA}, μg cm^{-3}) to that of the reacted α-pinene (Δ_{VOC}, μg cm^{-3}) in each experimental run.

$$Y = \frac{m_{SOA}}{\Delta_{VOC}} \quad (1)$$

where m_{SOA} was calculated assuming SOA density of 1.34 g cm^{-3} (Sato et al., 2018) and equal to the arithmetic mean of the last three data of each experimental run. It was corrected for wall loss using the bulk-volume wall-loss rate, assuming a first-order wall-loss constant which is independent of particle size and reaction time (Pathak et al., 2007b). The size-resolved wall-loss rates were not applied because the bulk wall-loss rates were very close to the size-resolved rates at approximately 300 nm (Fig. S2). The mode diameters of the volume-size distributions of the seed particles (Fig. S3) and volume-size distributions of aerosols at the end of the ozonolysis reactions were also approximately 300 nm (Fig. S3).

In addition, a four-product volatility basis-set (VBS) gas/particle partitioning absorption model (Eq. (2), Donahue et al., 2006; Lane et al., 2008) was applied to assist the interpretation of the observed responses of Y to the chamber temperature and the acidity of the seed aerosol.

$$Y = \sum_i \alpha_i \left(\frac{1}{1+c_i^*/m_{SOA}}\right) \quad (2)$$

where α_i is the mass-based stoichiometric yield for product i, and c_i^* is the effective saturation concentration of i in μg m^{-3}. In this study, α_i is assumed to be temperature-independent whereas the temperature dependence of c_i^* is accounted using the Clausius–Clapeyron equation as follows:

$$c_i^* = c_{i,0}^* \frac{T_0}{T} \exp\left(\frac{\Delta H_{vap,i}}{R}\left(\frac{1}{T_0} - \frac{1}{T}\right)\right) \quad (3)$$

https://doi.org/10.5194/acp-2020-798
Preprint. Discussion started: 17 September 2020

Atmospheric Chemistry and Physics Discussions

where T_0 is the reference temperature, which is 298 K in this study; $c^*_{i,0}$ is the effective saturation concentration of i at T_0; R is the ideal gas constant; and $\Delta H_{vap,i}$ is the effective enthalpy of vaporization. The temperature dependence of Y is then represented by the substitution of Eq. (3) for c^*_i in Eq. (2). We further assume a constant effective ΔH_{vap} for all condensable organic compounds. Thus, the four-product basis set has five free parameters: α_1, α_2, α_3, α_4, and ΔH_{vap}. Here, c^*_0 = {1, 10, 100, 1000} μg m^{-3}, which was set based on the measured range of m_{SOA} (Sect. 4.1) in this study. Microsoft Excel Solver GRG Nonlinear engine was used for the derivation of the five parameters under neutral or acidic seed aerosol conditions.

3.2 Volatility distribution analysis

SOA compounds identified from the six filter samples through LC-TOF-MS analysis were subjected to volatility distribution analysis. The saturation concentration (C^*) of each chemical compound was calculated then ascribed to the volatility basis-set (Donahue et al., 2006). Again, 298 K was used as the reference temperature (T_0). For compounds whose chemical structures have been suggested by previous researchers, the SPARC online calculator (Hilal et al., 2003; Sato et al., 2018) was used for the derivation of their C^*_0. For other compounds, including organosulfates, the following equation from Li et al. (2016) was applied:

$$\log_{10} C^*_0 = (n^0_C - n_C)b_C - n_O b_O - 2\frac{n_C n_O}{n_C + n_O} b_{CO} - n_S b_S \qquad (4)$$

where n^0_C is the reference carbon number; n_C, n_O, and n_S are the numbers of carbon, oxygen, and sulfur atoms in the molecule, respectively; b_C, b_O, and b_S are the respective contribution of each atom to $\log_{10} C^*_0$; and b_{CO} is the carbon–oxygen nonideality. For compounds containing only C, H, and O atoms, the values for n^0_C, b_C, b_O, and b_{CO} are 22.66, 0.4481, 1.656, and −0.7790, respectively. For OS compounds that contain C, H, O, and S atoms, the values for n^0_C, b_C, b_O, b_{CO}, and b_S are 24.06, 0.3637, 1.327, −0.3988, and 0.7579, respectively. The $\log_{10} C^*_0$ of the 362 compounds determined by LC-TOF-MS analysis are presented in Table S3.

4 Results and discussion

4.1 Temperature and acidity dependence of SOA yield

An example experimental run of SOA formation from α-pinene ozonolysis is presented in Fig. 1 (Exp. No. 27). The initial concentrations of α-pinene and ozone were 145 and >824 ppbv, respectively. The number concentration of seed aerosols was 9.6×10^3 cm^{-3} and they were concentrated in the diameter range of 80–200 nm. SOA was formed while α-pinene was consumed immediately at the introduction of excess O_3. The mass concentration of SOA reached its maximum while α-pinene was almost totally consumed approximately 50 min after the introduction of ozone. The time variation of α-pinene conforms to an α-pinene limited first-order chemical reaction (5τ = 47 min). With the wall-loss correction, the SOA loading at the end of this experiment was calculated to be 200 μg m^{-3}, which resulted in a final SOA yield of 26.3 % (Table S2). As the SOA concentration was kept constant after 50 min, we consider the wall-loss correction applied here was reasonable (Ng et al., 2006). Without wall-loss correction, the concentration of SOA at 90 min could be underestimated by approximately 40 %. The observed aerosol number-size distribution shifted to a much greater but narrower size range of 200–300 nm at the end of the experiment.

https://doi.org/10.5194/acp-2020-798
Preprint. Discussion started: 17 September 2020

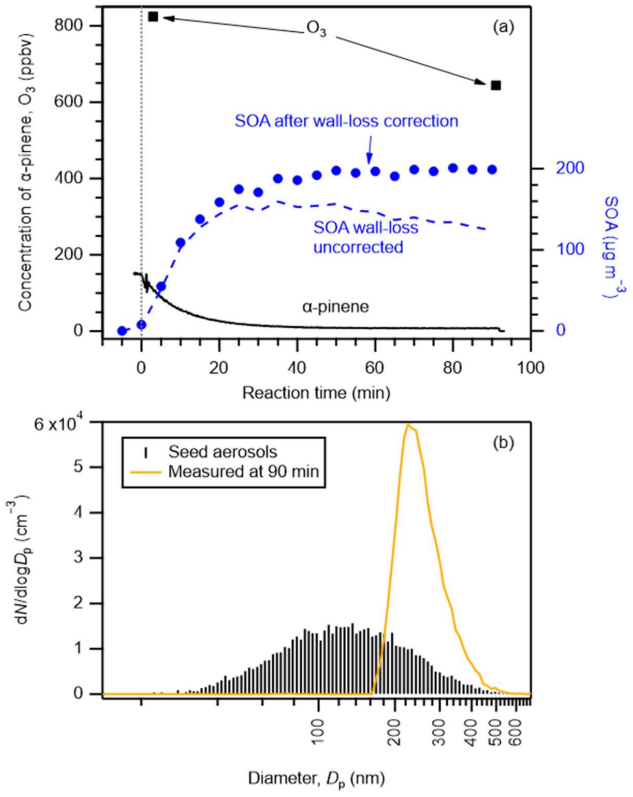

Figure 1: Example experimental run: (a) concentrations of α-pinene (black solid curve), O_3 (square markers), and SOA before (blue dashed line) and after (circle markers) wall-loss correction compared with reaction time; and (b) number-size distributions of seed aerosols (black sticks) and aerosols at the end of the experimental run (brown curve). The vertical dotted line in panel (a) indicates the starting time that O_3 was injected. Data shown in this figure are from Exp. No. 27 (Table S2).

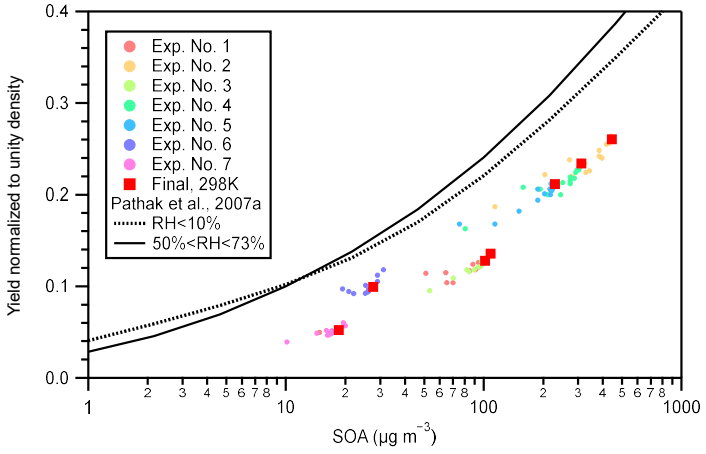

Figure 2: Yield comparison. SOA mass yields measured at 298 K under neutral seed conditions of this study were compared to that of Pathak et al. (2007a). Small circle markers represent the real time SOA yields, i.e., the SOA yields along with the α-pinene ozonolysis reactions from 0 to 90 min. Different experimental runs are differentiated by colors. Square markers represent the final SOA yields of the seven experiments. The curves present the four-product volatility basis-set fitting of α-pinene ozonolysis experiments under low NOx dark conditions summarized in Pathak et al. (2007a). The solid curve represents results under RH range of 50–73 % and the dotted curve represents results under RH<10 %. Note that all data presented in this figure were normalized to unity density (1 g cm^{-3}).

https://doi.org/10.5194/acp-2020-798
Preprint. Discussion started: 17 September 2020

Atmospheric Chemistry and Physics Discussions

The measured SOA mass yields at 298 K under neutral seed conditions were compared with that of Pathak et al. (2007a) (Fig. 2). In this study, seven experiments with varied initial α-pinene concentrations (54–323 ppbv) at 298 K under neutral seed conditions were conducted under the RH conditions of approximately 26–27 % (Table S1). In Pathak et al. (2007a), the SOA mass yields from pre-existing studies under low NOx dark ozonolysis conditions were summarized and categorized into two groups according to experimental RH conditions: RH<10 % and RH=50–73 %. They further fitted the data in each group using the multiple product basis-set approach (Pathak et al., 2007a). The four-product basis-set fitting was adopted to compare with the experiment results of this study (Fig. 2). The SOA yields in this study were 25–60 % lower than that of Pathak et al. (2007a). Possible reasons may include no consideration of the wall-loss of oxidized organic vapors because the surface to volume ratio of the chamber used in this study could be much greater than those of previous studies (the volume of the chamber used in this study is 0.7 m^3, whereas those of previous studies are 10–200 m^3 (Pathak et al., 2007a and references therein)). According to Zhang et al. (2014), the vapor wall-loss bias factor, R_{wall} (defined as the ratio of the SOA mass when the vapor wall loss was assumed to be zero, to the SOA mass when the optimal vapor wall loss rate was applied), was reported to be ~4 at the initial seed surface area of ~2 × 10^3 μm^2 cm^{-3} (seed-to-chamber surface area ratio ~1 × 10^{-3}) and ~2 at the initial seed surface area of >6 × 10^3 μm^2 cm^{-3} (seed-to-chamber surface area ratio >3 × 10^{-3}) during the photooxidation of toluene. As the initial seed surface area in the present study was in the range of (1−3) × 10^3 μm^2 cm^{-3} (seed-to-chamber surface area ratio (1−4) × 10^{-4}), R_{wall} in the Teflon bag might be at least twice that of the large chambers. This leads to the underestimation of the SOA yield of 50 % compared with the values obtained from the large chambers. We note that this is a shortcoming of the compact chamber with 0.7 m^3 volume used in this study. In the following paragraph, the temperature dependence of SOA yields will be discussed assuming that the underestimation of the SOA yield due to the wall-loss of oxidized organic vapors does not affect the temperature dependence.

The yields of SOA from α-pinene ozonolysis under different experimental conditions in this study are summarized in Fig. 3. Results under neutral and acidic seed conditions are presented separately in panels (a) and (b). In each panel, the measured SOA yields as a function of SOA mass loadings are indicated by markers and the four-product VBS model fitting results are shown by curves. The fitted parameters with the four-product VBS model under neutral and acidic seed conditions are summarized in Table 1. Under neutral seed conditions, the fitted temperature independent stoichiometric yields α = {0.00, 0.09, 0.09, 0.52} and ΔH_{vap} is 25 kJ mol^{-1}. Under acidic seed conditions, α = {0.00, 0.14, 0.05, 0.43} and ΔH_{vap} is 44 kJ mol^{-1}. The fitting results pointed out that most of the detected SOA compounds are of relatively high saturation concentration (i.e., c^* at 298 K of 1000 μg m^{-3}) under both neutral and acidic seed conditions. Weak increases of SOA yields with decreases of the chamber temperature can be observed under both seed conditions. This is consistent with the result in Pahtak et al. (2007b), which found a weak dependence of SOA yields on temperature in the range of 288–303 K. As temperature decreases, SVOCs tend to partition into the particle phase because of the lowering of their volatilities.

The effective ΔH_{vap} of α-pinene ozonolysis SOA derived from the four-product VBS fitting in this study was compared with previous studies (Table 2). The ΔH_{vap} values derived in this study were comparable to those in Saathoff et al. (2009) and Pathak et al. (2007a) where the experiments were executed in large chambers of 10–200 m^3. It may support our assumption that the temperature dependence of SOA yields was not influenced by vapor wall-loss. It is also in agreement with the ΔH_{vap} of 40 kJ mol^{-1} applied in the CMAQv4.7 model (Carlton et al., 2010). However, they are lower than that of Saha et al. (2016) and much lower than that of Epstein et al. (2010). While the ΔH_{vap} in Saha et al. (2016) was derived based on thermodeneuder measurements which attributed 20–40 % of SOA mass to low-volatility material (C^* < 0.3 μg m^{-3}), most of the measured SOA in this study are of relatively high volatility as aforementioned. The differences in the volatility of SOA and the derived ΔH_{vap} between Saha et al. (2016) and this study are consistent with the general phenomenon that ΔH_{vap} is conversely related with volatility (Epstein et al., 2010). The ΔH_{vap} in Epstein et al. (2010) was derived from published experimental vapor pressure

https://doi.org/10.5194/acp-2020-798
Preprint. Discussion started: 17 September 2020

Atmospheric Chemistry and Physics Discussions

data of organic compounds. The reason for the difference in ΔH_{vap} between this study and Epstein et al. (2010) cannot be currently explained.

The dependence of SOA yields on the acidity of seed particles seems to be small in this study. According to previous α-pinene ozonolysis studies, SOA yields can be enhanced under acidic seed particle conditions compared to neutral seed conditions (Czoschke et al., 2003; Gao et al., 2004; Iinuma et al., 2004, 2005; Czoschke and Jang, 2006; Jang et al., 2006; Northcross and Jang, 2007). But the degree of the enhancement seemed to be affected by the experimental settings. It is noted that all those previous studies except Gao et al. (2004) and Iinuma et al. (2005) did not use an OH radical scavenger, which plays an important role in influencing SOA yields (Iinuma et al., 2005; Na et al., 2007). In addition, the enhancement of SOA formation under acidic seed conditions can be influenced by the SOA mass loadings. This is probably because the SOA components can be of high viscosity under conditions when RH is smaller than around 50 %, and if high SOA mass loadings coated the seed particles, the acid-catalyzed heterogeneous SOA formation reactions could be impeded (Shiraiwa et al., 2013b; Zhou et al., 2013). In Gao et al. (2004), obvious initial α-pinene concentration dependence of the enhancement of SOA yields under acidic compared with neutral seed conditions was observed. For initial α-pinene concentrations of 12, 25, 48, 52, 96, 120, and 135 ppbv, the relative enhancements of SOA yields were 37, 34, 26, 24, 15, 10, and 8 %, respectively. This is consistent with the statement that viscous material hinders acid-catalyzed reactions. In this study, the initial concentrations of α-pinene were 54–323 ppbv at 298 K, suggesting that the enhancement could be less than 24 %. Although with a high uncertainty, the four-product VBS model fitting results from this study indicate that the SOA yields could have been enhanced under acidic seed conditions when the SOA mass loadings were low (Fig. S4). When SOA loadings were high, the enhancement disappeared (Fig. S4). When the SOA volume loading was 50 $\mu m^3\ cm^{-3}$, the fitted SOA yields under acidic conditions were enhanced by 11, 17, and 25 % compared to neutral seed conditions under 298, 288, and 278 K, respectively. This is consistent with Gao et al. (2004) and is also comparable to the results of Iinuma et al. (2005). In Iinuma et al. (2005), the experiment with 2-Butanol as an OH radical scavenger under room temperature (294–298 K) found an enhancement of 19 % with the final SOA volume concentration of approximately 50 $\mu m^3\ cm^{-3}$. Furthermore, the degree of acidity of the seed aerosols could also have influenced the enhancement (Gao et al., 2004; Czoschke and Jang, 2006). Further comprehensive studies are warranted (including the consideration of the aerosol viscosity and phase separation) on the influence of seed aerosol acidity on α-pinene ozonolysis SOA formation.

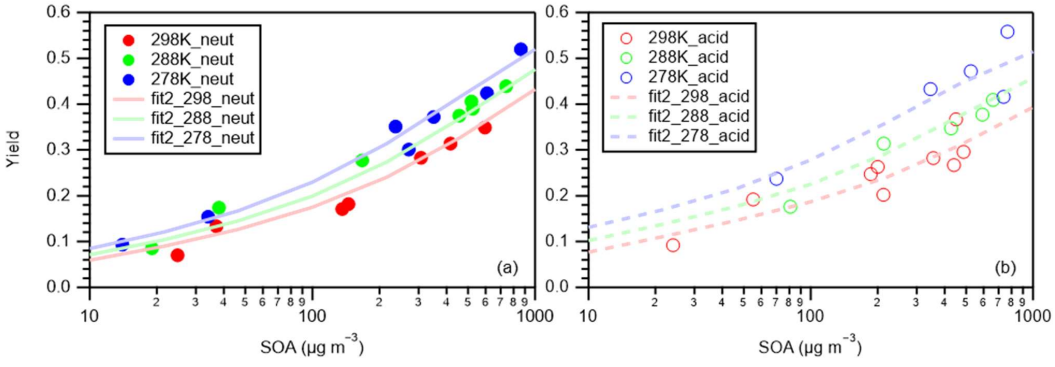

Figure 3: Mass yields of SOA for increasing SOA mass loadings. Markers are measured data and curves are fitting of measured data using a four-product VBS model (Donahue et al., 2006; Lane et al., 2008). Panel (a) presents results under neutral seed conditions, and panel (b) presents results under acidic seed conditions.

https://doi.org/10.5194/acp-2020-798
Preprint. Discussion started: 17 September 2020

Atmospheric Chemistry and Physics Discussions

Table 1: Four-product VBS model fitting results.

Seed particles	Temperature (K)	c^* values (μg m^{-3})				α (Stoichiometric Yields) values				ΔH_{vap} (kJ mol^{-1})
		c_1^*	c_2^*	c_3^*	c_4^*	α_1	α_2	α_3	α_4	
Neutral	298	1.000	10.00	100.0	1000	0.00	0.09	0.09	0.52	25
	288	0.7292	7.292	72.92	729.2					
	278	0.5191	5.191	51.91	519.1					
Acidic	298	1.000	10.00	100.0	1000	0.00	0.14	0.05	0.43	44
	288	0.5550	5.550	55.50	555.0					
	278	0.2949	2.949	29.49	294.9					

Table 2: Comparison of ΔH_{vap} in this study with previous studies.

References	ΔH_{vap} (kJ mol^{-1})	C^* ranges (μg m^{-3})	Temp ranges (°C)
This work; ozonolysis	25–44	10^1–10^3	5–25
Saha et al., 2016; ozonolysis	80−11 $\log_{10}C^*$	10^{-2}–10^4	30–120
Saathoff et al., 2009; ozonolysis	24–59	2.1×10^{-3}–56	−30–40
Pathak et al., 2007a; ozonolysis	30, 70	10^{-2}–10^4	0–49
Epstein et al., 2010; semiempirical correlation-based fit	129−11 $\log_{10}C^*$	10^{-2}–10^{10}	27

4.2 Temperature and acidity dependence of SOA composition

Among the 362 compounds identified through LC-ToF-MS analysis in this study (Table S3), 331 compounds were ascribed to VBS bin ranges of −8–3. The other 31 compounds were ascribed to higher VBS bin ranges of 4–6, which is unrealistic for the compounds in the aerosol phase. Additionally, those latter compounds only accounted for an average of 12 % of the total mass of identified compounds. Thus, only the former 331 compounds are targeted in the following discussions.

Figure 4 presents the volatility distributions of the identified compounds. The measured intensities of aerosol phase compounds were normalized by their total intensity for each experiment and are presented in Fig. 4a. Compounds that were attributed to VBS bins between 0 and 3 are known as SVOC (Li et al., 2016). Those in bins 2 and 3 generally presented a decreasing tendency with the increase of experimental temperatures, and there was no obvious temperature dependence for those in bins 0 and 1 (Fig. 4a). The corresponding gas phase concentrations of each compound were derived assuming gas-particle partitioning equilibrium (Odum et al., 1996). The ΔH_{vap} values derived in this study (Table 1) were used to calculate the saturation concentration under 278 and 288 K following Eq. (3). The intensity of both the aerosol and gas phases were then normalized by their total amount and are presented in Fig. 4b. With the inclusion of the corresponding gaseous phase compounds, the temperature dependence of compounds in VBS bin 3 changed to positive (i.e., increased with temperature) whereas the tendency in bin 2 remained negative (Fig. 4b). As the α-pinene ozonolysis rate constant does not vary much under the temperature range of 278–298 K (Akimoto, 2016) and α-pinene was completely consumed at the reaction time of 90 min, the total amount of formed SVOCs should be similar at the three temperatures. Hence, the total amounts of gas and aerosol phase compounds in each VBS bin should be independent of experimental temperatures. If a larger ΔH_{vap} were applied for the derivation of the intensity of gas phase compounds (e.g., the semiempirical equation in Epstein et al. (2010)), the total amount in VBS bin 3 at 298 K would be much higher than at other temperatures, which is unreasonable. This suggested the appropriateness of the ΔH_{vap} values derived from the four-product VBS fitting of the SOA yields in Sect. 4.1. In addition, we note that the volatility distribution pattern derived in this study is similar to that of the experimental runs 1 and 6 (derived using the same method) of Sato et al. (2018), although positive electrospray ionization analysis was used and the α-pinene ozonolysis experiments were carried out under dry conditions in the latter. In Fig. 4b, the volatility distributions determined from SOA yield curves were also presented. The mass fractions determined from the LC-TOF-MS data at VBS bins 1 and 3, and 0 and 2, were smaller and larger, respectively, than those determined from the SOA yield curves. These differences are probably

https://doi.org/10.5194/acp-2020-798
Preprint. Discussion started: 17 September 2020

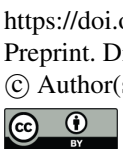

Atmospheric Chemistry and Physics Discussions

caused by uncertainties in saturation concentration and sensitivity parameterization as well as the existence of undetected molecules in the LC-TOF-MS analysis (Sato et al., 2018).

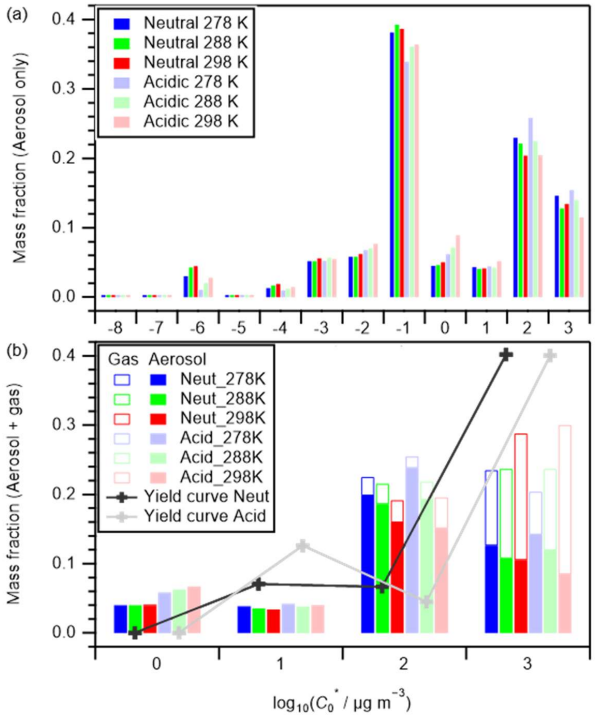

Figure 4: Volatility distributions of chemical components in (a) aerosol only phase and (b) aerosol + gas phases. In panel (a), data were normalized by the total signal intensity of the aerosol phase of each experiment; in panel (b), data were normalized by the total intensity of the aerosol phase and its equilibrium gas phase in each experiment. Curves and markers imposed in panel (b) are the volatility distributions under neutral (dark color) and acidic (light color) seed conditions determined from SOA yield curves (Sato et al., 2018).

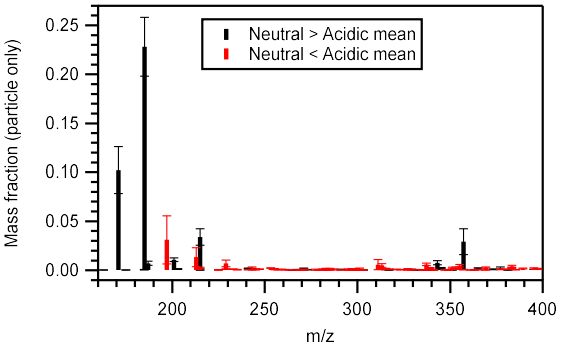

Figure 5: Mean aerosol phase mass fraction distributions of compounds whose aerosol phase mass fractions under acidic seed conditions were more than 1.1 (red symbols) or less than 0.9 (black symbols) times those of neutral seed conditions. Whiskers represent the standard deviations of the three experiments at different temperatures.

https://doi.org/10.5194/acp-2020-798
Preprint. Discussion started: 17 September 2020

Atmospheric Chemistry and Physics Discussions

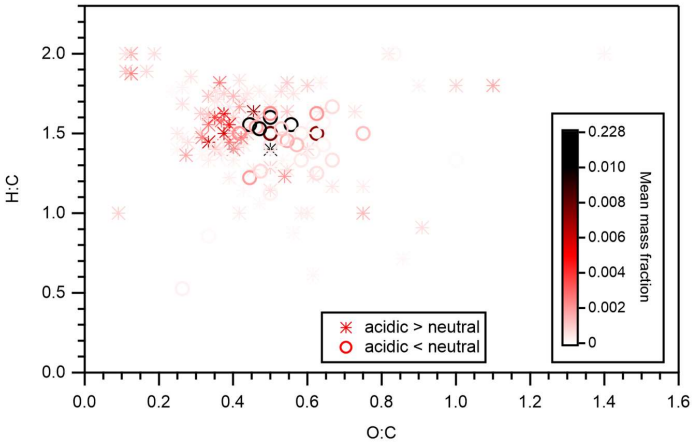

Figure 6: Atomic H to C ratio (H:C) versus O to C ratio (O:C). Star and Circle markers respectively indicate compounds whose aerosol phase mass fractions under acidic seed conditions were more than 1.1 and less than 0.9 times those of neutral seed conditions. Color scale indicates the mean mass fraction of identified compounds across all six experiments. Notably, organosulfates were not presented.

To gain more insights into the acidity dependence of the α-pinene ozonolysis SOA, the relative intensities of the compounds identified by LC-TOF-MS under acidic and neutral seed conditions were compared. For compounds whose intensity under acidic seed conditions was more than 1.1 times that of neutral seed conditions, monomers with a chemical formula of $C_{10}H_{9-18}O_{4-14}$ accounted for 32 % and oligomers with a chemical formula of $C_{11-22}H_{7-35}O_{2-12}$ accounted for 68 % of the total intensity. Conversely, for compounds whose intensity under acidic conditions was less than 0.9 times that of neutral seed conditions, monomers with a chemical formula of $C_{6-10}H_{7-15}O_{4-6}$ accounted for 87 % and oligomers with a chemical formula of $C_{11-21}H_{9-27}O_{5-10}$ accounted for 13 % of the total intensity.

Figure 5 presents the aerosol phase mass distributions of compounds whose mass fractions under acidic seed conditions were more than 1.1 (or less than 0.9) times those of neutral seed conditions. The molecular mass of those compounds with greater mass fractions under acidic seed conditions was generally distributed in the higher mass end compared with those with greater mass fractions under neutral seed conditions. The mass fraction weighted mean molecular mass of those compounds presented greater intensities under acidic seed conditions was 284 ± 14 (mean ± standard deviation) g mol^{-1}, whereas of those presented greater intensities under neutral seed conditions was 204 ± 4 g mol^{-1}.

Figure 6 presents the identified compounds whose intensity under acidic seed conditions was more than 1.1 (or less than 0.9) times that of neutral seed conditions in the atomic H to C ratio (H:C) versus O to C ratio (O:C) space. The color scale indicates the mean mass fraction of identified compounds across all six experiments. It is suggested that compounds with a lower intensity under acidic seed conditions were concentratedly distributed in the O:C ratio range of 0.4–0.75 and H:C ratio range of 1.1–1.7, whereas those with higher intensity under acidic seed conditions were more broadly distributed in the H:C versus O:C space. Compounds with O:C ratios less than 0.4 were oligomers with a chemical formula of $C_{11-22}H_{19-35}O_{2-7}$ and were distributed in the VBS bins of −3 to 3. Compounds with O:C ratios greater than 0.75 were likely to be highly oxidized molecules with a chemical formula of $C_{10-14}H_{9-21}O_{9-14}$, and were attributed to VBS bins −8 to −2. Furthermore, oligomers with O:C ratios of less than 0.4 accounted for 61 % of those oligomers with high relative intensity under acidic conditions, whereas those with O:C ratios of greater than 0.75 accounted for only 1 %. This, together with the aforementioned chemical formula and molecular mass distributions, indicated that the formation of many oligomers, especially with small O:C ratios, was enhanced under acidic seed conditions.

Figure 7 presents the compounds whose normalized intensity under acidic seed conditions was less than 0.9 (panel a) or more than 1.1 (panel b) times that of neutral seed conditions in the VBS space. The acidity dependence of the major compounds in

https://doi.org/10.5194/acp-2020-798
Preprint. Discussion started: 17 September 2020

Atmospheric Chemistry and Physics Discussions

VBS bins was tentatively explained from the viewpoints of acid-catalyzed decomposition reactions or acid-catalyzed heterogenous reactions. Compounds that presented lower intensities under acidic than neutral seed conditions were mainly distributed in VBS bins 3, 2, −1, −4, and −6 (Fig. 7a). The respective compounds that presented the highest intensity in VBS bins 3, 2, −1, −4, and −6 were m/z 215.091 ($C_{10}H_{15}O_5$), 171.065 ($C_8H_{11}O_4$), 185.081 ($C_9H_{13}O_4$), 343.139 ($C_{16}H_{23}O_8$), and 357.154 ($C_{17}H_{25}O_8$), and they accounted for on average 25, 46, 62, 54, and 99 % of the total intensity of the compounds determined in the respective bins. The structures of m/z 215 have been proposed by Zhang et al. (2017) as hydroperoxides from α-pinene ozonolysis reactions. They can be decomposed under acidic seed conditions to m/z 197.081 ($C_{10}H_{13}O_4$, VBS bin 2) (Scheme 1a) as well as m/z 155.010 ($C_8H_{11}O_3$, VBS bin 5) (Scheme 1b) (acid-catalyzed decomposition of hydroperoxides; Seubold and Vaughan, 1953). Next, previous studies indicate that m/z 171 and 185 were monomer precursors of dimers m/z 343 and 357, and all four products exist in both laboratory α-pinene ozonolysis SOA samples and field samples (Gao et al., 2004; Yasmeen et al., 2010; Kristensen et al., 2014; Zhang et al., 2015). The chemical structure of m/z 185 has been proposed as pinic acid (Gao et al., 2004; Yasmeen et al., 2010; Kristensen et al., 2014), and m/z 171 as terpenylic acid (Yasmeen et al., 2010; Kristensen et al., 2014) and norpinic acid (Gao et al., 2004). In this study, excess OH scavengers could have minimized the formation of an OH functional group in the α-pinene ozonolysis products whereas the aldehydes should dominate the products (Gaona-Colmán et al., 2017). Thus, it is possible that the acid-catalyzed heterogenous esterification between acid products such as m/z 171 and 185, and aldehyde products such as pinonaldehyde (Hallquist et al., 2009), led to the decreased intensity of m/z 171 and 185 under acidic seed conditions, which further led to the decreased intensity of the related dimers of m/z 343 and 357. Scheme 2 presents a possible esterification reaction between terpenylic acid (a possible isomer of m/z 171) and pinonaldehyde. The product, m/z 339.180 ($C_{18}H_{27}O_6$), ascribed to VBS bin −1, presented higher relative intensity under acidic seed conditions.

The compounds with higher contributions under acidic than neutral seed conditions were mainly distributed in VBS bins −3, −2, 0 and 2 (Fig. 7b). The most abundant compounds of those whose intensity under acidic seed conditions was more than 1.1 times that of neutral conditions in bins 2, −2, and −3 were m/z 197 ($C_{10}H_{13}O_4$), 355.175 ($C_{18}H_{27}O_7$), and 383.170 ($C_{19}H_{27}O_8$), respectively. Their contributions to the total signal of their respective bins were 14, 7, and 5 %, and the ratios of their intensities under acidic seed conditions to those under neutral seed conditions were 5.4, 1.8, and 1.3, respectively. The higher intensity of m/z 197 under acidic than neutral conditions might be explained partly by the acid-catalyzed decomposition of m/z 215 (Scheme 1a). Zhang et al. (2015) proposed m/z 355 as a dimer ester with a hydroperoxide function. Another possible assignment of m/z 355 is an ester from the reaction of a Criegee intermediate ($C_{10}H_{16}O_3$) with terpenylic acid and/or norpinic acid ($C_8H_{12}O_4$) (Kristensen et al., 2017). The latter assignment of the product also has a hydroperoxide group. The formation of hydroperoxides involving Criegee intermediates has been observed in the gas phase (Sekimoto et al., 2020) and on the surface of aqueous droplets (Enami et al., 2017). The relatively high intensity of m/z 355 under acidic seed conditions might be explained by the fact that the hydrolysis of ester hydroperoxides becomes slower under acidic conditions (Zhao et al., 2018). Kristensen et al. (2017) proposed m/z 383 as a dimer ester, whereas the molecular structure is to be identified. In bin 0, the intensities of m/z 311.149 ($C_{16}H_{23}O_6$) and m/z 313.165 ($C_{16}H_{25}O_6$) were the highest (contributing on average 10 and 9 % of the total intensity of the bin, respectively), and under acidic seed conditions were 4.8 and 1.5 times those of neutral seed conditions, respectively. Although the structure of m/z 311 is yet to be identified, m/z 313 was proposed as a dimer ester by Zhang et al. (2015). These dimer esters at m/z 383 and 313 might be formed through acid-catalyzed heterogeneous reactions.

In addition, the eleven identified organosulfate compounds were ascribed to the VBS bins of −3 to 0 (Table 3). All of them presented greater intensity on average under acidic conditions than under neutral seed conditions (Fig. S5). Four of the OS were in VBS bin 0, which together contributed 9.2 % of the intensity of that bin. The contributions of the two, three, and two OS compounds (which respectively belongs to VBS bins of −1, −2, and −3) to their respective bins were 0.4, 4.7, and 2.6 %. The formation mechanisms of those OS compounds will be discussed in the next section. It should be noted that the estimated

https://doi.org/10.5194/acp-2020-798
Preprint. Discussion started: 17 September 2020

Atmospheric Chemistry and Physics Discussions

intensities of OS compounds in this study might be of a high uncertainty because methanol, which could react with carbonyl and carboxylic compounds in the SOA (Bateman et al., 2008), was used as the extraction solution. Acetonitrile should be used as the extraction solution in future studies to confirm the influence (Bateman et al., 2008).

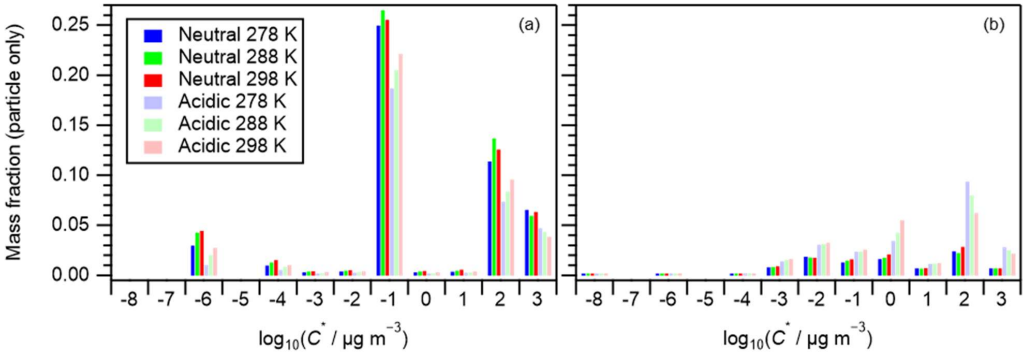

Figure 7: Volatility distribution of SOA compounds whose aerosol phase mass fractions under acidic seed conditions were (a) less than 0.9 and (b) more than 1.1 times those of neutral seed conditions. Note the mass fractions presented here are same as those in Fig. 4a.

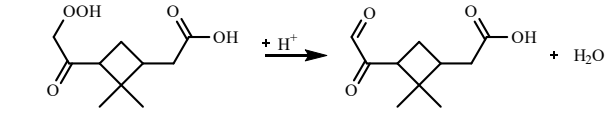

(a)

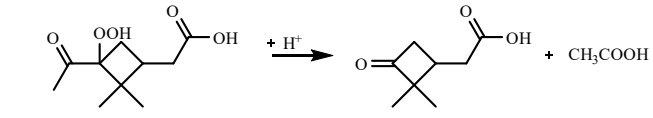

(b)

Scheme 1: Proposed acid-catalyzed decomposition reactions of hydroperoxides at m/z 215 in this study.

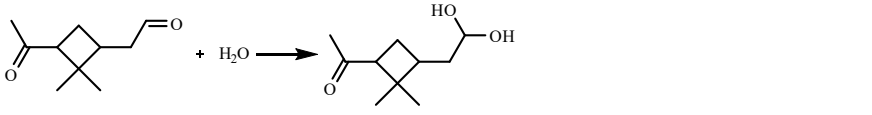

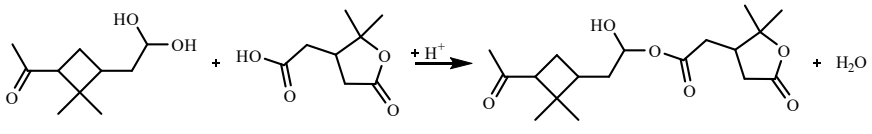

Scheme 2: Possible acid-catalyzed esterification reaction of Terpenylic acid (m/z 171) with Pinonaldehyde.

4.3 OS formation under acidic conditions

In this study, significant signals were identified for eleven organosulfates under acidic seed conditions (Fig. S5). Figure 8 presents the molecular yields of those OS compounds estimated from the LC-TOF-MS analysis. M/z 223 was the most abundant OS identified at 298 k, followed by m/z 279, 281, 269, 283, 265, 253, 267, 251, 249, and 247.

The possible formation mechanisms of the OS compounds were proposed based on previous literatures combined with the experimental settings of this study. To our knowledge, while the formation of OS through α-pinene ozonolysis in the

https://doi.org/10.5194/acp-2020-798
Preprint. Discussion started: 17 September 2020

Atmospheric Chemistry and Physics Discussions

presence of an OH radical scavenger has been reported very recently (Ye et al., 2018; Stangl et al., 2019; Wang et al., 2019), these studies focused on the reactions between α-pinene ozonolysis products with SO_2 rather the identification of OS compounds. Earlier studies on the identification and formation mechanisms of OS with α-pinene as the precursor VOC related to photooxidation (i.e., OH-initiated oxidation) or nighttime oxidation (i.e., NO_3-initiated oxidation under dark conditions) (Surratt et al., 2007, 2008). In this study, the formation of OS from α-pinene ozonolysis in the presence of an OH radical scavenger and acidic seed aerosols was investigated.

Table 3 summarizes the possible chemical structures of the eleven detected OS compounds and their precursor α-pinene oxidation products. Among the eleven OS compounds detected in this study, eight of them have been detected in previous laboratory and/or field studies of α-pinene oxidations (Table 3), and the other three (m/z 251, 253, and 269) were detected for the first time in this study. While all eleven OS compounds detected in this study were very likely from α-pinene ozonolysis reaction because the presence of excess OH scavenger in this study, five of the previously identified OS compounds (m/z 223, 247, 249, 265, and 279) were detected in α-pinene photooxidation and/or nighttime oxidation experiments (Surratt et al., 2008) and the other three (m/z 267, 281, and 283) were only identified in ambient aerosol.

The chemical structures of five of the OS compounds (i.e., m/z 223, 247, 249, 265, and 279) have been proposed in previous studies. Four of them (m/z 223, 249, and 279) were likely to be sulfate esters formed from alcohols and sulfate (Surratt et al., 2007, 2008; Zhang et al., 2015; Hettiyadura et al., 2019), and one (m/z 265) was from the sulfacation of the aldehyde compound, specifically pinonaldehyde (Liggio and Li, 2006; Surratt et al., 2007). The former is referred hereafter as the alcohol pathway, and the latter the aldehyde pathway (aldehyde + HSO_4^-; Surratt et al., 2007). Because aldehydes should dominate the products from α-pinene ozonolysis in the presence of an OH scavenger (Gaona-Colmán et al., 2017) and pinonaldehyde has been detected in previous α-pinene ozonolysis studies with an OH scavenger (Jackson et al., 2017), we propose that the aldehyde pathway could be one of the dominant OS formation pathways in this study. In addition to m/z 265, we propose possible aldehyde precursors formed in α-pinene ozonolysis experiments for five other OS compounds identified in this study (i.e., m/z 251, 253, 269, 279, and 283). Except for the study where the aldehyde precursor of m/z 269 was found (Reinnig et al., 2009), an OH scavenger was used in all other studies where the aldehyde precursors were found (Yu et al., 1999; Ma et al., 2008; Jackson et al., 2017). Presently, we suppose that the other five OS compounds were possibly formed through the alcohol pathway although no relevant information has been found for m/z 247 and 249. Notably, another possible precursor with a hydroxyl function, which is formed in α-pinene ozonolysis experiments with an OH scavenger, has also been found for the OS at m/z 269 (Kristensen et al., 2014). Additionally, the proposed precursor for m/z 283 (Table 3) also contains a hydroxyl function, which can form another OS of m/z 265.038 ($C_9H_{13}O_7S$) through the alcohol pathway. A weak signal of this OS was observed (not presented in Fig. S5).

As shown in Fig. 8, the yields of m/z 247, 249, and 265 decreased with the increase of temperature. Conversely, the yields of other OS compounds increased with the temperature, or at least the yields at 278 K were the lowest among the three temperature conditions. The temperature dependence of OS yields seems not to be directly related to the formation mechanisms of either the alcohol pathway or the aldehyde pathway. It should be noted that the OS at m/z 247 and 249 could only be observed at relatively low temperatures. As eleven OS (including three unreported) were observed in the α-pinene ozonolysis reaction with an OH scavenger and acidic seed particles, the identification of the structure of these OS using high-resolution ion mobility mass spectrometry is planned for the next step. When the structure of the OS can be determined and the precursor compound can be expected, the formation mechanism of the OS in α-pinene ozonolysis with acidic seeds will be confirmed.

https://doi.org/10.5194/acp-2020-798
Preprint. Discussion started: 17 September 2020

Atmospheric Chemistry and Physics Discussions

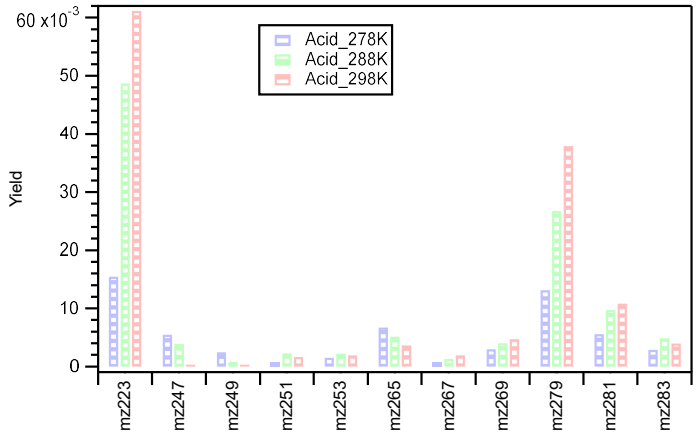

Figure 8: Molecular yields of the eleven OS compounds under acidic seed conditions at different temperatures. The time window used for the calculation of the intensity of each OS compound is indicated in Fig. S5.

495

https://doi.org/10.5194/acp-2020-798
Preprint. Discussion started: 17 September 2020

Atmospheric Chemistry and Physics Discussions

Table 3: Organosulfates identified in this study, their respective m/z and formula of $[M-H]^-$, assigned VBS bin number, proposed OS structure, and proposed precursor oxidation product structure.

m/z $[M-H]^-$	Formula $[M-H]^-$	VBS bin	Proposed OS structure (this study)		Proposed precursor (this study)		Previously proposed OS structure	Previously proposed precursor	Ref.[a]
			Aldehyde + HSO_4^-	Esterification	Aldehyde + HSO_4^-	Esterification			
223.027	$C_7H_{11}O_6S^-$	0	-	-	-	-	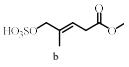 b	-	bcd
247.063	$C_{10}H_{15}O_5S^-$	0	-	-	-	-	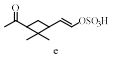 e	-	cfg
249.079	$C_{10}H_{17}O_5S^-$	0	-	-	-	-	 c	 c	cgh
251.060	$C_9H_{15}O_6S^-$	0		-	 i	-	-	-	This study
253.039	$C_8H_{13}O_7S^-$	−1		-	 i	-	-	-	This study
265.074	$C_{10}H_{17}O_6S^-$	−1	Same as previous	-	Same as previous	-	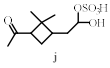 j	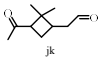 jk	cgl
267.017	$C_8H_{11}O_8S^-$	−2	-	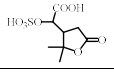	-	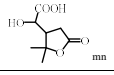 mn	-	-	o
269.033	$C_8H_{13}O_8S^-$	−2		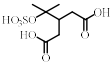	 p	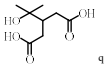 q	-	-	This study
279.053	$C_{10}H_{15}O_7S^-$	−2	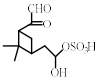	-	 i	-	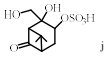 j or 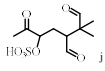 j or 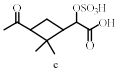 c	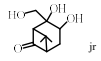 jr or 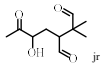 jr or 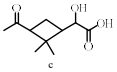 c	cgj
281.033	$C_9H_{13}O_8S^-$	−3	-	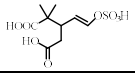	-	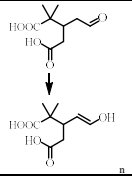 n	-	-	stu
283.048	$C_9H_{15}O_8S^-$	−3		 (m/z=265)	 v	-	-	-	cs

[a]Selected laboratory and/or field studies where the corresponding OS has been identified; [b]Hettiyadura et al., 2019; [c]Surratt et al., 2008; [d]Yassine et al., 2012; [e]Zhang et al., 2015; [f]Tao et al., 2014; [g]Ma et al., 2014; [h]Wang et al., 2018b; [i]Yu et al., 1999; [j]Surratt et al., 2007; [k]Jackson et al., 2017; [l]Liggio and Li, 2006; [m]Kahnt et al., 2014a; [n]Kahnt et al., 2014b; [o]Meade et al., 2016; [p]Reinnig et al., 2009; [q]Kristensen et al., 2014; [r]Aschmann et al., 1998, 2002; [s]Brüggemann et al., 2019; [t]Wang et al., 2016; [u]Brüggemann et al., 2017; [v]Ma et al., 2008.

https://doi.org/10.5194/acp-2020-798
Preprint. Discussion started: 17 September 2020

Atmospheric Chemistry and Physics Discussions

5 Summary and conclusions

A temperature controllable chamber system has been developed for studying SOA formation. In this study, SOA formation from α-pinene ozonolysis was studied with diethyl ether as an OH radical scavenger at temperatures of 278, 288, and 298 K under acidic/neutral seed conditions. The SOA yields and compounds with a molecular mass of less than 400 Da determined by a LC-TOF-MS were analyzed from the perspectives of temperature and seed particle acidity dependence.

The SOA yield slightly increased with the decrease of chamber temperature. The enthalpy of vaporization in neutral and acidic seed conditions was estimated to be 25 and 44 kJ mol^{-1}, respectively. The acidity dependence of the SOA yield at low SOA loadings was comparable to those reported in Gao et al. (2004) and Iinuma et al. (2005).

Among the 362 identified compounds, the volatility of 331 was distributed in the VBS bins between −8 and 3. The temperature dependence of the volatility distribution of those identified compounds (particle phase + gas phase) could be consistently explained by the enthalpy of vaporization derived in this study.

The compounds whose intensities under acidic seed conditions were less than 0.9 times those of neutral seed conditions were dominated by monomers, whereas the compounds whose intensities under acidic seed conditions were more than 1.1 times those of neutral seed conditions were dominated by oligomers. The O:C ratios of the former were concentrated in the range of 0.4–0.75. The O:C ratios of the latter were broadly distributed. The compounds with O:C ratios less than 0.4 were all oligomers that accounted for 61 % of the oligomers with high relative intensity under acidic conditions, whereas those with O:C ratios of greater than 0.75 were highly oxidized molecules and only contributed to 1 % of those oligomers. In addition, the mean molecular mass of the former compounds (204 ± 4 g mol^{-1}) were evidently lower than those of the latter (284 ± 14 g mol^{-1}). These differences indicated that the formation of many oligomers, especially with small O:C ratios, was enhanced under acidic seed conditions. The acidity-dependence of certain major compounds might be explained by acid-catalyzed heterogenous reactions (e.g., m/z 171, 185, 343, and 357) or acid-catalyzed decomposition reactions (e.g., m/z 215 and 197).

For the first time, organosulfate compounds were studied for α-pinene ozonolysis reaction at the presence of an OH scavenger and acidic seed aerosols. Eleven OS compounds were determined from LC-TOF-MS analysis. All of them on average presented a higher yield under acidic than neutral seed conditions. Six of those OS compounds were possibly formed through the aldehyde + HSO_4^- pathway, which should be confirmed in future studies through high resolution mass spectrometry analysis.

Data availability.

All the final data supporting the findings of this study are available in the manuscript or in the supplement. Raw data used to derive the final data are available on request to the corresponding author.

Author contributions

SI, YD, SE, and HT did chamber experiments; KS and SR did LC-TOF-MS analyses; SI, YD, SE, and MY did data analyses; YD, SI, and HT made the manuscript; and all authors contributed to the revisions of the manuscript.

Competing interests.

The authors declare no competing interests.

https://doi.org/10.5194/acp-2020-798
Preprint. Discussion started: 17 September 2020

Atmospheric Chemistry and Physics Discussions

Acknowledgements

We thank Ms. Sumiko Komori, Dr. Yoshikatsu Takazawa, and Dr. Tomoharu Sano for the technical support. This work was supported by NIES research funding (Type A) and JSPS KAKENHI Grant No. 19H01154.

References

Akimoto, H.: Atmospheric Reaction Chemistry, 1 ed., Springer Atmospheric Sciences, Springer Japan, Tokyo, Japan, XVI, 433 pp., doi:10.1007/978-4-431-55870-5, 2016.

Aschmann, S. M., Reissell, A., Atkinson, R., and Arey, J.: Products of the gas phase reactions of the OH radical with alpha- and beta-pinene in the presence of NO, Journal of Geophysical Research-Atmospheres, 103, 25553-25561, doi:10.1029/98jd01676, 1998.

Aschmann, S. M., Atkinson, R., and Arey, J.: Products of reaction of OH radicals with alpha-pinene, Journal of Geophysical Research-Atmospheres, 107, doi:10.1029/2001jd001098, 2002.

Bateman, A. P., Walser, M. L., Desyaterik, Y., Laskin, J., Laskin, A., and Nizkorodov, S. A.: The effect of solvent on the analysis of secondary organic aerosol using electrospray ionization mass spectrometry, Environmental Science & Technology, 42, 7341-7346, doi:10.1021/es801226w, 2008.

Bruggemann, M., Poulain, L., Held, A., Stelzer, T., Zuth, C., Richters, S., Mutzel, A., van Pinxteren, D., Iinuma, Y., Katkevica, S., Rabe, R., Herrmann, H., and Hoffmann, T.: Real-time detection of highly oxidized organosulfates and BSOA marker compounds during the F-BEACh 2014 field study, Atmospheric Chemistry and Physics, 17, 1453-1469, doi:10.5194/acp-17-1453-2017, 2017.

Bruggemann, M., van Pinxteren, D., Wang, Y. C., Yu, J. Z., and Herrmann, H.: Quantification of known and unknown terpenoid organosulfates in PM10 using untargeted LC-HRMS/MS: contrasting summertime rural Germany and the North China Plain, Environmental Chemistry, 16, 333-346, doi:10.1071/en19089, 2019.

Capouet, M., Mueller, J. F., Ceulemans, K., Compernolle, S., Vereecken, L., and Peeters, J.: Modeling aerosol formation in alpha-pinene photo-oxidation experiments, Journal of Geophysical Research-Atmospheres, 113, doi:10.1029/2007jd008995, 2008.

Carlton, A. G., Bhave, P. V., Napelenok, S. L., Edney, E. D., Sarwar, G., Pinder, R. W., Pouliot, G. A., and Houyoux, M.: Model Representation of Secondary Organic Aerosol in CMAQv4.7, Environmental Science & Technology, 44, 8553-8560, doi:10.1021/es100636q, 2010.

Chu, S. H., Paisie, J. W., and Jang, B. W. L.: PM data analysis - a comparison of two urban areas: Fresno and Atlanta, Atmospheric Environment, 38, 3155-3164, doi:10.1016/j.atmosenv.2004.03.018, 2004.

Czoschke, N. M., Jang, M., and Kamens, R. M.: Effect of acidic seed on biogenic secondary organic aerosol growth, Atmospheric Environment, 37, 4287-4299, doi:10.1016/s1352-2310(03)00511-9, 2003.

Czoschke, N. M., and Jang, M. S.: Acidity effects on the formation of alpha-pinene ozone SOA in the presence of inorganic seed, Atmospheric Environment, 40, 4370-4380, doi:10.1016/j.atmosenv.2006.03.030, 2006.

Donahue, N. M., Robinson, A. L., Stanier, C. O., and Pandis, S. N.: Coupled partitioning, dilution, and chemical aging of semivolatile organics, Environmental Science & Technology, 40, 2635-2643, doi:10.1021/es052297c, 2006.

Duporté, G., Flaud, P. M., Geneste, E., Augagneur, S., Pangui, E., Lamkaddam, H., Gratien, A., Doussin, J. F., Budzinski, H., Villenave, E., and Perraudin, E.: Experimental Study of the Formation of Organosulfates from alpha-Pinene Oxidation. Part I: Product Identification, Formation Mechanisms and Effect of Relative Humidity, Journal of Physical Chemistry A, 120, 7909-7923, doi:10.1021/acs.jpca.6b08504, 2016.

Duporté, G., Flaud, P. M., Kammer, J., Geneste, E., Augagneur, S., Pangui, E., Lamkaddam, H., Gratien, A., Doussin, J. F., Budzinski, H., Villenave, E., and Perraudin, E.: Experimental Study of the Formation of Organosulfates from alpha-Pinene Oxidation. 2. Time Evolution and Effect of Particle Acidity, Journal of Physical Chemistry A, 124, 409-421, doi:10.1021/acs.jpca.9b07156, 2020.

Eddingsaas, N. C., Loza, C. L., Yee, L. D., Chan, M., Schilling, K. A., Chhabra, P. S., Seinfeld, J. H., and Wennberg, P. O.: alpha-pinene photooxidation under controlled chemical conditions - Part 2: SOA yield and composition in low- and high-NOx environments, Atmospheric Chemistry and Physics, 12, 7413-7427, doi:10.5194/acp-12-7413-2012, 2012.

Ehn, M., Thornton, J. A., Kleist, E., Sipila, M., Junninen, H., Pullinen, I., Springer, M., Rubach, F., Tillmann, R., Lee, B., Lopez-Hilfiker, F., Andres, S., Acir, I. H., Rissanen, M., Jokinen, T., Schobesberger, S., Kangasluoma, J., Kontkanen, J., Nieminen, T., Kurten, T., Nielsen, L. B., Jorgensen, S., Kjaergaard, H. G., Canagaratna, M., Dal Maso, M., Berndt, T., Petaja, T., Wahner, A., Kerminen, V. M., Kulmala, M., Worsnop, D. R., Wildt, J., and Mentel, T. F.: A large source of low-volatility secondary organic aerosol, Nature, 506, 476-479, doi:10.1038/nature13032, 2014.

https://doi.org/10.5194/acp-2020-798
Preprint. Discussion started: 17 September 2020

Atmospheric Chemistry and Physics Discussions

Enami, S., and Colussi, A. J.: Criegee Chemistry on Aqueous Organic Surfaces, Journal of Physical Chemistry Letters, 8, 1615-1623, doi:10.1021/acs.jpclett.7b00434, 2017.

Epstein, S. A., Riipinen, I., and Donahue, N. M.: A Semiempirical Correlation between Enthalpy of Vaporization and Saturation Concentration for Organic Aerosol, Environmental Science & Technology, 44, 743-748, doi:10.1021/es902497z, 2010.

Gao, S., Ng, N. L., Keywood, M., Varutbangkul, V., Bahreini, R., Nenes, A., He, J. W., Yoo, K. Y., Beauchamp, J. L., Hodyss, R. P., Flagan, R. C., and Seinfeld, J. H.: Particle phase acidity and oligomer formation in secondary organic aerosol, Environmental Science & Technology, 38, 6582-6589, doi:10.1021/es049125k, 2004.

Gaona-Colman, E., Blanco, M. B., Barnes, I., Wiesen, P., and Teruel, M. A.: OH- and O-3-initiated atmospheric degradation of camphene: temperature dependent rate coefficients, product yields and mechanisms, Rsc Advances, 7, 2733-2744, doi:10.1039/c6ra26656h, 2017.

Guenther, A. B., Jiang, X., Heald, C. L., Sakulyanontvittaya, T., Duhl, T., Emmons, L. K., and Wang, X.: The Model of Emissions of Gases and Aerosols from Nature version 2.1 (MEGAN2.1): an extended and updated framework for modeling biogenic emissions, Geoscientific Model Development, 5, 1471-1492, doi:10.5194/gmd-5-1471-2012, 2012.

Hallquist, M., Wenger, J. C., Baltensperger, U., Rudich, Y., Simpson, D., Claeys, M., Dommen, J., Donahue, N. M., George, C., Goldstein, A. H., Hamilton, J. F., Herrmann, H., Hoffmann, T., Iinuma, Y., Jang, M., Jenkin, M. E., Jimenez, J. L., Kiendler-Scharr, A., Maenhaut, W., McFiggans, G., Mentel, T. F., Monod, A., Prevot, A. S. H., Seinfeld, J. H., Surratt, J. D., Szmigielski, R., and Wildt, J.: The formation, properties and impact of secondary organic aerosol: current and emerging issues, Atmospheric Chemistry and Physics, 9, 5155-5236, doi:10.5194/acp-9-5155-2009, 2009.

Hettiyadura, A. P. S., Al-Naiema, I. M., Hughes, D. D., Fang, T., and Stone, E. A.: Organosulfates in Atlanta, Georgia: anthropogenic influences on biogenic secondary organic aerosol formation, Atmospheric Chemistry and Physics, 19, 3191-3206, doi:10.5194/acp-19-3191-2019, 2019.

Hilal, S. H., Karickhoff, S. W., and Carreira, L. A.: Prediction of the vapor pressure boiling point, heat of vaporization and diffusion coefficient of organic compounds, Qsar & Combinatorial Science, 22, 565-574, doi:10.1002/qsar.200330812, 2003.

Hinkley, J. T., Bridgman, H. A., Buhre, B. J. P., Gupta, R. P., Nelson, P. F., and Wall, T. F.: Semi-quantitative characterisation of ambient ultrafine aerosols resulting from emissions of coal fired power stations, Science of the Total Environment, 391, 104-113, doi:10.1016/j.scitotenv.2007.10.017, 2008.

Iinuma, Y., Boge, O., Gnauk, T., and Herrmann, H.: Aerosol-chamber study of the alpha-pinene/O-3 reaction: influence of particle acidity on aerosol yields and products, Atmospheric Environment, 38, 761-773, doi:10.1016/j.atmosenv.2003.10.015, 2004.

Iinuma, Y., Boge, O., Miao, Y., Sierau, B., Gnauk, T., and Herrmann, H.: Laboratory studies on secondary organic aerosol formation from terpenes, Faraday Discussions, 130, 279-294, doi:10.1039/b502160j, 2005.

Iinuma, Y., Muller, C., Boge, O., Gnauk, T., and Herrmann, H.: The formation of organic sulfate esters in the limonene ozonolysis secondary organic aerosol (SOA) under acidic conditions, Atmospheric Environment, 41, 5571-5583, doi:10.1016/j.atmosenv.2007.03.007, 2007.

Iinuma, Y., Boge, O., Kahnt, A., and Herrmann, H.: Laboratory chamber studies on the formation of organosulfates from reactive uptake of monoterpene oxides, Physical Chemistry Chemical Physics, 11, 7985-7997, doi:10.1039/b904025k, 2009.

Jackson, S. R., Ham, J. E., Harrison, J. C., and Wells, J. R.: Identification and quantification of carbonyl-containing alpha-pinene ozonolysis products using O-tert-butylhydroxylamine hydrochloride, Journal of Atmospheric Chemistry, 74, 325-338, doi:10.1007/s10874-016-9344-6, 2017.

Jang, M., Czoschke, N. M., Northcross, A. L., Cao, G., and Shaof, D.: SOA formation from partitioning and heterogeneous reactions: Model study in the presence of inorganic species, Environmental Science & Technology, 40, 3013-3022, doi:10.1021/es0511220, 2006.

Jang, M., Cao, G., and Paul, J.: Colorimetric particle acidity analysis of secondary organic aerosol coating on submicron acidic aerosols, Aerosol Science and Technology, 42, 409-420, doi:10.1080/02786820802154861, 2008.

Jang, M. S., Czoschke, N. M., Lee, S., and Kamens, R. M.: Heterogeneous atmospheric aerosol production by acid-catalyzed particle-phase reactions, Science, 298, 814-817, doi:10.1126/science.1075798, 2002.

Kahnt, A., Iinuma, Y., Blockhuys, F., Mutzel, A., Vermeylen, R., Kleindienst, T. E., Jaoui, M., Offenberg, J. H., Lewandowski, M., Boge, O., Herrmann, H., Maenhaut, W., and Claeys, M.: 2-Hydroxyterpenylic Acid: An Oxygenated Marker Compound for alpha-Pinene Secondary Organic Aerosol in Ambient Fine Aerosol, Environmental Science & Technology, 48, 4901-4908, doi:10.1021/es500377d, 2014a.

Kahnt, A., Iinuma, Y., Mutzel, A., Boge, O., Claeys, M., and Herrmann, H.: Campholenic aldehyde ozonolysis: a mechanism leading to specific biogenic secondary organic aerosol constituents, Atmospheric Chemistry and Physics, 14, 719-736, doi:10.5194/acp-14-719-2014, 2014b.

https://doi.org/10.5194/acp-2020-798
Preprint. Discussion started: 17 September 2020

Atmospheric Chemistry and Physics Discussions

645 Kelly, J. M., Doherty, R. M., O'Connor, F. M., and Mann, G. W.: The impact of biogenic, anthropogenic, and biomass burning volatile organic compound emissions on regional and seasonal variations in secondary organic aerosol, Atmospheric Chemistry and Physics, 18, 7393-7422, doi:10.5194/acp-18-7393-2018, 2018.

Kristensen, K., Cui, T., Zhang, H., Gold, A., Glasius, M., and Surratt, J. D.: Dimers in alpha-pinene secondary organic aerosol: effect of hydroxyl radical, ozone, relative humidity and aerosol acidity, Atmospheric Chemistry and Physics, 14, 4201-4218, 650 doi:10.5194/acp-14-4201-2014, 2014.

Kristensen, K., Jensen, L. N., Glasius, M., and Bilde, M.: The effect of sub-zero temperature on the formation and composition of secondary organic aerosol from ozonolysis of alpha-pinene, Environmental Science-Processes & Impacts, 19, 1220-1234, doi:10.1039/c7em00231a, 2017.

Lane, T. E., Donahue, N. M., and Pandis, S. N.: Simulating secondary organic aerosol formation using the volatility basis-set 655 approach in a chemical transport model, Atmospheric Environment, 42, 7439-7451, doi:10.1016/j.atmosenv.2008.06.026, 2008.

Lewandowski, M., Jaoui, M., Kleindienst, T. E., Offenberg, J. H., and Edney, E. O.: Composition of PM2.5 during the summer of 2003 in Research Triangle Park, North Carolina, Atmospheric Environment, 41, 4073-4083, doi:10.1016/j.atmosenv.2007.01.012, 2007.

660 Li, Y., Poschl, U., and Shiraiwa, M.: Molecular corridors and parameterizations of volatility in the chemical evolution of organic aerosols, Atmospheric Chemistry and Physics, 16, 3327-3344, doi:10.5194/acp-16-3327-2016, 2016.

Liggio, J., and Li, S. M.: Organosulfate formation during the uptake of pinonaldehyde on acidic sulfate aerosols, Geophysical Research Letters, 33, L13808, doi:10.1029/2006gl026079, 2006.

Ma, Y., Russell, A. T., and Marston, G.: Mechanisms for the formation of secondary organic aerosol components from the 665 gas-phase ozonolysis of alpha-pinene, Physical Chemistry Chemical Physics, 10, 4294-4312, doi:10.1039/b803283a, 2008.

Ma, Y., Xu, X. K., Song, W. H., Geng, F. H., and Wang, L.: Seasonal and diurnal variations of particulate organosulfates in urban Shanghai, China, Atmospheric Environment, 85, 152-160, doi:10.1016/j.atmosenv.2013.12.017, 2014.

Meade, L. E., Riva, M., Blomberg, M. Z., Brock, A. K., Qualters, E. M., Siejack, R. A., Ramakrishnan, K., Surratt, J. D., and Kautzman, K. E.: Seasonal variations of fine particulate organosulfates derived from biogenic and anthropogenic hydrocarbons 670 in the mid-Atlantic United States, Atmospheric Environment, 145, 405-414, doi:10.1016/j.atmosenv.2016.09.028, 2016.

Messina, P., Lathiere, J., Sindelarova, K., Vuichard, N., Granier, C., Ghattas, J., Cozic, A., and Hauglustaine, D. A.: Global biogenic volatile organic compound emissions in the ORCHIDEE and MEGAN models and sensitivity to key parameters, Atmospheric Chemistry and Physics, 16, 14169-14202, doi:10.5194/acp-16-14169-2016, 2016.

Na, K., Song, C., Switzer, C., and Cocker, D. R.: Effect of ammonia on secondary organic aerosol formation from alpha-675 Pinene ozonolysis in dry and humid conditions, Environmental Science & Technology, 41, 6096-6102, doi:10.1021/es061956y, 2007.

Ng, N. L., Kroll, J. H., Keywood, M. D., Bahreini, R., Varutbangkul, V., Flagan, R. C., Seinfeld, J. H., Lee, A., and Goldstein, A. H.: Contribution of first- versus second-generation products to secondary organic aerosols formed in the oxidation of biogenic hydrocarbons, Environmental Science & Technology, 40, 2283-2297, doi:10.1021/es052269u, 2006.

680 Northcross, A. L., and Jang, M.: Heterogeneous SOA yield from ozonolysis of monoterpenes in the presence of inorganic acid, Atmospheric Environment, 41, 1483-1493, doi:10.1016/j.atmosenv.2006.10.009, 2007.

Nozière, B., Ekstrom, S., Alsberg, T., and Holmstrom, S.: Radical-initiated formation of organosulfates and surfactants in atmospheric aerosols, Geophysical Research Letters, 37, doi:10.1029/2009gl041683, 2010.

Odum, J. R., Hoffmann, T., Bowman, F., Collins, D., Flagan, R. C., and Seinfeld, J. H.: Gas/particle partitioning and secondary 685 organic aerosol yields, Environmental Science & Technology, 30, 2580-2585, doi:10.1021/es950943+, 1996.

Offenberg, J. H., Lewandowski, M., Edney, E. O., Kleindienst, T. E., and Jaoui, M.: Influence of Aerosol Acidity on the Formation of Secondary Organic Aerosol from Biogenic Precursor Hydrocarbons, Environmental Science & Technology, 43, 7742-7747, doi:10.1021/es901538e, 2009.

Parrish, D. D., Singh, H. B., Molina, L., and Madronich, S.: Air quality progress in North American megacities: A review, 690 Atmospheric Environment, 45, 7015-7025, doi:10.1016/j.atmosenv.2011.09.039, 2011.

Pathak, R. K., Presto, A. A., Lane, T. E., Stanier, C. O., Donahue, N. M., and Pandis, S. N.: Ozonolysis of alpha-pinene: parameterization of secondary organic aerosol mass fraction, Atmospheric Chemistry and Physics, 7, 3811-3821, doi:10.5194/acp-7-3811-2007, 2007a.

Pathak, R. K., Stanier, C. O., Donahue, N. M., and Pandis, S. N.: Ozonolysis of alpha-pinene at atmospherically relevant 695 concentrations: Temperature dependence of aerosol mass fractions (yields), Journal of Geophysical Research-Atmospheres, 112, doi:10.1029/2006jd007436, 2007b.

https://doi.org/10.5194/acp-2020-798
Preprint. Discussion started: 17 September 2020

Peltier, R. E., Sullivan, A. P., Weber, R. J., Brock, C. A., Wollny, A. G., Holloway, J. S., de Gouw, J. A., and Warneke, C.: Fine aerosol bulk composition measured on WP-3D research aircraft in vicinity of the Northeastern United States - results from NEAQS, Atmospheric Chemistry and Physics, 7, 3231-3247, doi:10.5194/acp-7-3231-2007, 2007.

Reinnig, M. C., Warnke, J., and Hoffmann, T.: Identification of organic hydroperoxides and hydroperoxy acids in secondary organic aerosol formed during the ozonolysis of different monoterpenes and sesquiterpenes by on-line analysis using atmospheric pressure chemical ionization ion trap mass spectrometry, Rapid Communications in Mass Spectrometry, 23, 1735-1741, doi:10.1002/rcm.4065, 2009.

Rengarajan, R., Sudheer, A. K., and Sarin, M. M.: Aerosol acidity and secondary organic aerosol formation during wintertime over urban environment in western India, Atmospheric Environment, 45, 1940-1945, doi:10.1016/j.atmosenv.2011.01.026, 2011.

Riva, M., Tomaz, S., Cui, T. Q., Lin, Y. H., Perraudin, E., Gold, A., Stone, E. A., Villenave, E., and Surratt, J. D.: Evidence for an Unrecognized Secondary Anthropogenic Source of Organosulfates and Sulfonates: Gas-Phase Oxidation of Polycyclic Aromatic Hydrocarbons in the Presence of Sulfate Aerosol, Environmental Science & Technology, 49, 6654-6664, doi:10.1021/acs.est.5b00836, 2015.

Riva, M., Barbosa, T. D., Lin, Y. H., Stone, E. A., Gold, A., and Surratt, J. D.: Chemical characterization of organosulfates in secondary organic aerosol derived from the photooxidation of alkanes, Atmospheric Chemistry and Physics, 16, 11001-11018, doi:10.5194/acp-16-11001-2016, 2016.

Saathoff, H., Naumann, K. H., Mohler, O., Jonsson, A. M., Hallquist, M., Kiendler-Scharr, A., Mentel, T. F., Tillmann, R., and Schurath, U.: Temperature dependence of yields of secondary organic aerosols from the ozonolysis of alpha-pinene and limonene, Atmospheric Chemistry and Physics, 9, 1551-1577, doi:10.5194/acp-9-1551-2009, 2009.

Saha, P. K., and Grieshop, A. P.: Exploring Divergent Volatility Properties from Yield and Thermodenuder Measurements of Secondary Organic Aerosol from alpha-Pinene Ozonolysis, Environmental Science & Technology, 50, 5740-5749, doi:10.1021/acs.est.6b00303, 2016.

Sato, K., Hatakeyama, S., and Imamura, T.: Secondary organic aerosol formation during the photooxidation of toluene: NOx dependence of chemical composition, Journal of Physical Chemistry A, 111, 9796-9808, doi:10.1021/jp071419f, 2007.

Sato, K., Fujitani, Y., Inomata, S., Morino, Y., Tanabe, K., Ramasamy, S., Hikida, T., Shimono, A., Takami, A., Fushimi, A., Kondo, Y., Imamura, T., Tanimoto, H., and Sugata, S.: Studying volatility from composition, dilution, and heating measurements of secondary organic aerosols formed during alpha-pinene ozonolysis, Atmospheric Chemistry and Physics, 18, 5455-5466, doi:10.5194/acp-18-5455-2018, 2018.

Sato, K., Fujitani, Y., Inomata, S., Morino, Y., Tanabe, K., Hikida, T., Shimono, A., Takami, A., Fushimi, A., Kondo, Y., Imamura, T., Tanimoto, H., and Sugata, S.: A study of volatility by composition, heating, and dilution measurements of secondary organic aerosol from 1,3,5-trimethylbenzene, Atmospheric Chemistry and Physics, 19, 14901-14915, doi:10.5194/acp-19-14901-2019, 2019.

Sekimoto, K., Fukuyama, D., and Inomata, S.: Accurate identification of dimers from alpha-pinene oxidation using high-resolution collision-induced dissociation mass spectrometry, Journal of Mass Spectrometry, 55, e4508, 10.1002/jms.4508, 2020.

Seubold, F. H., and Vaughan, W. E.: Acid-catalyzed decomposition of cumene hydroperoxide, Journal of the American Chemical Society, 75, 3790-3792, doi:10.1021/ja01111a055, 1953.

Shiraiwa, M., Yee, L. D., Schilling, K. A., Loza, C. L., Craven, J. S., Zuend, A., Ziemann, P. J., and Seinfeld, J. H.: Size distribution dynamics reveal particle-phase chemistry in organic aerosol formation, Proceedings of the National Academy of Sciences of the United States of America, 110, 11746-11750, doi:10.1073/pnas.1307501110, 2013a.

Shiraiwa, M., Zuend, A., Bertram, A. K., and Seinfeld, J. H.: Gas-particle partitioning of atmospheric aerosols: interplay of physical state, non-ideal mixing and morphology, Physical Chemistry Chemical Physics, 15, 11441-11453, doi:10.1039/c3cp51595h, 2013b.

Shiraiwa, M., Ueda, K., Pozzer, A., Lammel, G., Kampf, C. J., Fushimi, A., Enami, S., Arangio, A. M., Frohlich-Nowoisky, J., Fujitani, Y., Furuyama, A., Lakey, P. S. J., Lelieveld, J., Lucas, K., Morino, Y., Poschl, U., Takaharna, S., Takami, A., Tong, H. J., Weber, B., Yoshino, A., and Sato, K.: Aerosol Health Effects from Molecular to Global Scales, Environmental Science & Technology, 51, 13545-13567, doi:10.1021/acs.est.7b04417, 2017.

Shrivastava, M., Cappa, C. D., Fan, J. W., Goldstein, A. H., Guenther, A. B., Jimenez, J. L., Kuang, C., Laskin, A., Martin, S. T., Ng, N. L., Petaja, T., Pierce, J. R., Rasch, P. J., Roldin, P., Seinfeld, J. H., Shilling, J., Smith, J. N., Thornton, J. A., Volkamer, R., Wang, J., Worsnop, D. R., Zaveri, R. A., Zelenyuk, A., and Zhang, Q.: Recent advances in understanding secondary organic aerosol: Implications for global climate forcing, Reviews of Geophysics, 55, 509-559, doi:10.1002/2016rg000540, 2017.

Stangl, C. M., Krasnomowitz, J. M., Apsokardu, M. J., Tiszenkel, L., Ouyang, Q., Lee, S., and Johnston, M. V.: Sulfur Dioxide Modifies Aerosol Particle Formation and Growth by Ozonolysis of Monoterpenes and Isoprene, Journal of Geophysical Research-Atmospheres, 124, 4800-4811, doi:10.1029/2018jd030064, 2019.

https://doi.org/10.5194/acp-2020-798
Preprint. Discussion started: 17 September 2020

Stocker, T. F., Qin, D. H., Plattner, G. K., Alexander, L. V., Allen, S. K., Bindoff, N. L., Breon, F. M., Church, J. A., Cubasch, U., Emori, S., Forster, P., Friedlingstein, P., Gillett, N., Gregory, J. M., Hartmann, D. L., Jansen, E., Kirtman, B., Knutti, R., Kanikicharla, K. K., Lemke, P., Marotzke, J., Masson-Delmotte, V., Meehl, G. A., Mokhov, II, Piao, S. L., Ramaswamy, V., Randall, D., Rhein, M., Rojas, M., Sabine, C., Shindell, D., Talley, L. D., Vaughan, D. G., and Xie, S. P.: Technical Summary, Climate Change 2013: the Physical Science Basis, 33-115, 2013.

Surratt, J. D., Kroll, J. H., Kleindienst, T. E., Edney, E. O., Claeys, M., Sorooshian, A., Ng, N. L., Offenberg, J. H., Lewandowski, M., Jaoui, M., Flagan, R. C., and Seinfeld, J. H.: Evidence for organosulfates in secondary organic aerosol, Environmental Science & Technology, 41, 517-527, doi:10.1021/es062081q, 2007.

Surratt, J. D., Gomez-Gonzalez, Y., Chan, A. W. H., Vermeylen, R., Shahgholi, M., Kleindienst, T. E., Edney, E. O., Offenberg, J. H., Lewandowski, M., Jaoui, M., Maenhaut, W., Claeys, M., Flagan, R. C., and Seinfeld, J. H.: Organosulfate formation in biogenic secondary organic aerosol, Journal of Physical Chemistry A, 112, 8345-8378, doi:10.1021/jp802310p, 2008.

Takahama, S., Davidson, C. I., and Pandis, S. N.: Semicontinuous measurements of organic carbon and acidity during the Pittsburgh air quality study: Implications for acid-catalyzed organic aerosol formation, Environmental Science & Technology, 40, 2191-2199, doi:10.1021/es050856+, 2006.

Tanner, R. L., Olszyna, K. J., Edgerton, E. S., Knipping, E., and Shaw, S. L.: Searching for evidence of acid-catalyzed enhancement of secondary organic aerosol formation using ambient aerosol data, Atmospheric Environment, 43, 3440-3444, doi:10.1016/j.atmosenv.2009.03.045, 2009.

Tao, S., Lu, X., Levac, N., Bateman, A. P., Nguyen, T. B., Bones, D. L., Nizkorodov, S. A., Laskin, J., Laskin, A., and Yang, X.: Molecular Characterization of Organosulfates in Organic Aerosols from Shanghai and Los Angeles Urban Areas by Nanospray-Desorption Electrospray Ionization High-Resolution Mass Spectrometry, Environmental Science & Technology, 48, 10993-11001, doi:10.1021/es5024674, 2014.

Tilmes, S., Hodzic, A., Emmons, L. K., Mills, M. J., Gettelman, A., Kinnison, D. E., Park, M., Lamarque, J. F., Vitt, F., Shrivastava, M., Campuzano-Jost, P., Jimenez, J. L., and Liu, X.: Climate Forcing and Trends of Organic Aerosols in the Community Earth System Model (CESM2), Journal of Advances in Modeling Earth Systems, 11, 4323-4351, doi:10.1029/2019ms001827, 2019.

Wang, N. X., Jorga, S. D., Pierce, J. R., Donahue, N. M., and Pandis, S. N.: Particle wall-loss correction methods in smog chamber experiments, Atmospheric Measurement Techniques, 11, 6577-6588, doi:10.5194/amt-11-6577-2018, 2018a.

Wang, S. Y., Zhou, S. M., Tao, Y., Tsui, W. G., Ye, J. H., Yu, J. Z., Murphy, J. G., McNeill, V. F., Abbatt, J. P. D., and Chan, A. W. H.: Organic Peroxides and Sulfur Dioxide in Aerosol: Source of Particulate Sulfate, Environmental Science & Technology, 53, 10695-10704, doi:10.1021/acs.est.9b02591, 2019.

Wang, X. K., Rossignol, S., Ma, Y., Yao, L., Wang, M. Y., Chen, J. M., George, C., and Wang, L.: Molecular characterization of atmospheric particulate organosulfates in three megacities at the middle and lower reaches of the Yangtze River, Atmospheric Chemistry and Physics, 16, 2285-2298, doi:10.5194/acp-16-2285-2016, 2016.

Wang, Y. J., Hu, M., Guo, S., Wang, Y. C., Zheng, J., Yang, Y. D., Zhu, W. F., Tang, R. Z., Li, X., Liu, Y., Le Breton, M., Du, Z. F., Shang, D. J., Wu, Y. S., Wu, Z. J., Song, Y., Lou, S. R., Hallquist, M., and Yu, J. Z.: The secondary formation of organosulfates under interactions between biogenic emissions and anthropogenic pollutants in summer in Beijing, Atmospheric Chemistry and Physics, 18, 10693-10713, doi:10.5194/acp-18-10693-2018, 2018b.

Yasmeen, F., Vermeylen, R., Szmigielski, R., Iinuma, Y., Boge, O., Herrmann, H., Maenhaut, W., and Claeys, M.: Terpenylic acid and related compounds: precursors for dimers in secondary organic aerosol from the ozonolysis of alpha- and beta-pinene, Atmospheric Chemistry and Physics, 10, 9383-9392, doi:10.5194/acp-10-9383-2010, 2010.

Yassine, M. M., Dabek-Zlotorzynska, E., Harir, M., and Schmitt-Kopplin, P.: Identification of Weak and Strong Organic Acids in Atmospheric Aerosols by Capillary Electrophoresis/Mass Spectrometry and Ultra-High-Resolution Fourier Transform Ion Cyclotron Resonance Mass Spectrometry, Analytical Chemistry, 84, 6586-6594, doi:10.1021/ac300798g, 2012.

Ye, J. H., Abbatt, J. P. D., and Chan, A. W. H.: Novel pathway of SO2 oxidation in the atmosphere: reactions with monoterpene ozonolysis intermediates and secondary organic aerosol, Atmospheric Chemistry and Physics, 18, 5549-5565, doi:10.5194/acp-18-5549-2018, 2018.

Yu, J. Z., Cocker, D. R., Griffin, R. J., Flagan, R. C., and Seinfeld, J. H.: Gas-phase ozone oxidation of monoterpenes: Gaseous and particulate products, Journal of Atmospheric Chemistry, 34, 207-258, doi:10.1023/a:1006254930583, 1999.

Zhang, Q., Jimenez, J. L., Worsnop, D. R., and Canagaratna, M.: A case study of urban particle acidity and its influence on secondary organic aerosol, Environmental Science & Technology, 41, 3213-3219, doi:10.1021/es061812j, 2007.

Zhang, X., Cappa, C. D., Jathar, S. H., McVay, R. C., Ensberg, J. J., Kleeman, M. J., and Seinfeld, J. H.: Influence of vapor wall loss in laboratory chambers on yields of secondary organic aerosol, Proceedings of the National Academy of Sciences of the United States of America, 111, 5802-5807, doi:10.1073/pnas.1404727111, 2014.

https://doi.org/10.5194/acp-2020-798
Preprint. Discussion started: 17 September 2020

Atmospheric Chemistry and Physics Discussions

Zhang, X., McVay, R. C., Huang, D. D., Dalleska, N. F., Aumont, B., Flagan, R. C., and Seinfeld, J. H.: Formation and evolution of molecular products in alpha-pinene secondary organic aerosol, Proceedings of the National Academy of Sciences of the United States of America, 112, 14168-14173, doi:10.1073/pnas.1517742112, 2015.

Zhang, X., Lambe, A. T., Upshur, M. A., Brooks, W. A., Be, A. G., Thomson, R. J., Geiger, F. M., Surratt, J. D., Zhang, Z. F., Gold, A., Graf, S., Cubison, M. J., Groessl, M., Jayne, J. T., Worsnop, D. R., and Canagaratna, M. R.: Highly Oxygenated Multifunctional Compounds in alpha-Pinene Secondary Organic Aerosol, Environmental Science & Technology, 51, 5932-5940, doi:10.1021/acs.est.6b06588, 2017.

Zhao, R., Kenseth, C. M., Huang, Y. L., Dalleska, N. F., Kuang, X. B. M., Chen, J. R., Paulson, S. E., and Seinfeld, J. H.: Rapid Aqueous-Phase Hydrolysis of Ester Hydroperoxides Arising from Criegee Intermediates and Organic Acids, Journal of Physical Chemistry A, 122, 5190-5201, doi:10.1021/acs.jpca.8b02195, 2018.

Zhou, S. M., Shiraiwa, M., McWhinney, R. D., Poschl, U., and Abbatt, J. P. D.: Kinetic limitations in gas-particle reactions arising from slow diffusion in secondary organic aerosol, Faraday Discussions, 165, 391-406, doi:10.1039/c3fd00030c, 2013.

Zhou, S. Z., Wang, Z., Gao, R., Xue, L. K., Yuan, C., Wang, T., Gao, X. M., Wang, X. F., Nie, W., Xu, Z., Zhang, Q. Z., and Wang, W. X.: Formation of secondary organic carbon and long-range transport of carbonaceous aerosols at Mount Heng in South China, Atmospheric Environment, 63, 203-212, doi:10.1016/j.atmosenv.2012.09.021, 2012.